Organisation for Economic Co-operation and Development

ENV/JM/MONO(2020)23

Unclassified English - Or. English

24 September 2020

ENVIRONMENT DIRECTORATE
JOINT MEETING OF THE CHEMICALS COMMITTEE AND THE WORKING PARTY ON CHEMICALS, PESTICIDES AND BIOTECHNOLOGY

# CASE STUDY ON THE USE OF INTEGRATED APPROACHES TO TESTING AND ASSESSMENT FOR MITOCHONDRIAL COMPLEX-III-MEDIATED NEUROTOXICITY OF AZOXYSTROBIN - READ-ACROSS TO OTHER STROBILURINS

**Series on Testing and Assessment**
**No. 327**

The corresponding annexes are available under the following cotes:
ENV/JM/MONO(2020)23/ANN1

**JT03465713**

**OECD Environment, Health and Safety Publications**

**Series on Testing and Assessment**

**No. 327**

# CASE STUDY ON THE USE OF INTEGRATED APPROACHES TO TESTING AND ASSESSMENT FOR MITOCHONDRIAL COMPLEX-III-MEDIATED NEUROTOXICITY OF AZOXYSTROBIN - READ-ACROSS TO OTHER STROBILURINS

IOMC INTER-ORGANIZATION PROGRAMME FOR THE SOUND MANAGEMENT OF CHEMICALS

A cooperative agreement among FAO, ILO, UNDP, UNEP, UNIDO, UNITAR, WHO, World Bank and OECD

**Environment Directorate**

**ORGANISATION FOR ECONOMIC CO-OPERATION AND DEVELOPMENT**

Paris 2020

# About the OECD

The Organisation for Economic Co-operation and Development (OECD) is an intergovernmental organisation in which representatives of 37 industrialised countries in North and South America, Europe and the Asia and Pacific region, as well as the European Commission, meet to co-ordinate and harmonise policies, discuss issues of mutual concern, and work together to respond to international problems. Most of the OECD's work is carried out by more than 200 specialised committees and working groups composed of member country delegates. Observers from several countries with special status at the OECD, and from interested international organisations, attend many of the OECD's workshops and other meetings. Committees and working groups are served by the OECD Secretariat, located in Paris, France, which is organised into directorates and divisions.

The Environment, Health and Safety Division publishes free-of-charge documents in twelve different series: **Testing and Assessment; Good Laboratory Practice and Compliance Monitoring; Pesticides; Biocides; Risk Management; Harmonisation of Regulatory Oversight in Biotechnology; Safety of Novel Foods and Feeds; Chemical Accidents; Pollutant Release and Transfer Registers; Emission Scenario Documents; Safety of Manufactured Nanomaterials;** and **Adverse Outcome Pathways**. More information about the Environment, Health and Safety Programme and EHS publications is available on the OECD's World Wide Web site (www.oecd.org/chemicalsafety/).

*This publication was developed in the IOMC context. The contents do not necessarily reflect the views or stated policies of individual IOMC Participating Organisations.*

The Inter-Organisation Programme for the Sound Management of Chemicals (IOMC) was established in 1995 following recommendations made by the 1992 UN Conference on Environment and Development to strengthen co-operation and increase international co-ordination in the field of chemical safety. The Participating Organisations are FAO, ILO, UNDP, UNEP, UNIDO, UNITAR, WHO, World Bank and OECD. The purpose of the IOMC is to promote co-ordination of the policies and activities pursued by the Participating Organisations, jointly or separately, to achieve the sound management of chemicals in relation to human health and the environment.

**This publication is available electronically, at no charge.**

**Also published in the Series on testing and Assessment link**

**For this and many other Environment,**
**Health and Safety publications, consult the OECD's**
**World Wide Web site www.oecd.org/chemicalsafety/**

**or contact:**

**OECD Environment Directorate,**
**Environment, Health and Safety Division**
**2, rue André-Pascal**
**75775 Paris cedex 16**
**France**
**Fax : (33-1) 44 30 61 80**
**E-mail : ehscont@oecd.org**

# Forward

OECD member countries have been making efforts to expand the use of alternative methods in assessing chemicals. The OECD has been developing guidance documents and tools for the use of alternative methods such as (Q)SAR, chemical categories and Adverse Outcome Pathways (AOPs) as a part of Integrated Approaches for Testing and Assessment (IATA). There is a need for the investigation of the practical applicability of these methods/tools for different aspects of regulatory decision-making, and to build upon case studies and assessment experience across jurisdictions.

The objective of the IATA Case Studies Project is to increase experience with the use of IATA by developing case studies, which constitute examples of predictions that are fit for regulatory use. The aim is to create common understanding of using novel methodologies and the generation of considerations/guidance stemming from these case studies.

This case study was developed by the EU ToxRisk project team (BIAC) for illustrating practical use of IATA and submitted to the 2019 review cycle of the IATA Case Studies Project. This case study was reviewed by the project team. The document was endorsed at the 4th meeting of the Working Party on Hazard Assessment in June 2020.

The following case study was also reviewed in the project in 2019:

1. CASE STUDY ON USE OF AN INTEGRATED APPROACH TO TESTING AND ASSESSMENT (IATA) AND NEW APPROACH METHODS TO INFORM A THEORETICAL READ-ACROSS FOR DERMAL EXPOSURE TO PROPYLPARABEN FROM COSMETICS, ENV/JM/MONO(2020)16.
2. CASE STUDY ON THE USE OF INTEGRATED APPROACHES FOR TESTING AND ASSESSMENT FOR SYSTEMIC TOXICITY ARISING FROM COSMETIC EXPOSURE TO CAFFEINE, ENV/JM/MONO(2020)17.
3. CASE STUDY ON THE USE OF INTEGRATED APPROACHES FOR TESTING AND ASSESSMENT FOR 90-DAY RAT ORAL REPEATED-DOSE TOXICITY OF CHLOROBENZENE-RELATED CHEMICALS, ENV/JM/MONO(2020)18.
4. CASE STUDY ON THE USE OF INTEGRATED APPROACHES FOR TESTING AND ASSESSMENT TO INFORM READ-ACROSS OF P-ALKYLPHENOLS: REPEATED-DOSE TOXICITY, ENV/JM/MONO(2020)19.
5. CASE STUDY ON THE USE OF INTEGRATED APPROACHES TO TESTING AND ASSESSMENT FOR PREDICTION OF A 90 DAY REPEATED DOSE TOXICITY STUDY (OECD 408) FOR 2-ETHYLBUTYRIC ACID USING A READ-ACROSS APPROACH FROM OTHER BRANCHED CARBOXYLIC ACIDS, ENV/JM/MONO(2020)20.
6. CASE STUDY ON THE USE OF INTEGRATED APPROACHES TO TESTING AND ASSESSMENT FOR READ-ACROSS BASED FILLING OF DEVELOPMENTAL TOXICITY DATA GAP FOR METHYL HEXANOIC ACID, ENV/JM/MONO(2020)21.

7. CASE STUDY ON THE USE OF INTEGRATED APPROACHES TO TESTING AND ASSESSMENT FOR IDENTIFICATION AND CHARACTERISATION OF PARKINSONIAN HAZARD LIABILITY OF DEGUELIN BY AN AOP-BASED TESTING AND READ ACROSS APPROACH, ENV/JM/MONO(2020)22.

These case studies are illustrative examples, and their publication as OECD monographs does not translate into direct acceptance of the methodologies for regulatory purposes across OECD countries. In addition, these cases studies should not be interpreted as official regulatory decisions made by the authoring member countries.

In addition, a considerations document summarising the learnings and lessons of the review experience of the case studies is published with the case studies:

REPORT ON CONSIDERATIONS FROM CASE STUDIES ON INTEGRATED APPROACHES FOR TESTING AND ASSESSMENT (IATA) -Fifth Review Cycle (2019) -, ENV/JM/MONO(2020)24.

This document is published under the responsibility of the Joint Meeting of the Chemicals Committee and Working Party on Chemicals, Pesticides and Biotechnology.

# Abstract

The synthetic strobilurin fungicides are derived from the naturally occurring strobilurin A and B. The strobilurins bind to the quinol oxidation site of cytochrome b of complex III (CIII) of the mitochondria which is also their fungicidal mode of action. There are some signals of potential neurotoxicity from *in vitro* studies by a CIII-mediated mechanism.

The objective of this case is to, by means of NAM data, to characterise the potential CIII-mediated neurotoxicity of azoxystrobin by read-across. The source compounds are other strobilurin fungicides. The formation of the category is based on the hypothesis that the compounds share similar chemical structure, similar pesticidal mode of action, similar toxicophore, similar neurotoxic potential and similar toxicokinetics to azoxystrobin. The source compounds chosen were pyraclostrobin, picoxystrobin, trifloxystrobin, and kresoxim-methyl. Furthermore, *in vitro* testing was conducted on Antimycin A, a well-established CIII inhibitor with neurotoxic effects, which serves as a reference compound for this mode of action. The degree of *in vivo* inhibition of the mitochondrial respiratory system depends on the respiratory activity and thus the tissues like brain can be more susceptible if exposed.

Existing regulatory *in vivo* data was collected for the source and target compounds with a focus on ADME, neurotoxicity as well as target organ toxicity data. The source compounds do neither show signs of neurotoxicity in neurotoxicity studies nor in other repeat dose toxicity studies.

The scientific hypothesis is: Can the absence of a neurotoxic potential (as detected with a TG424 study) mediated by inhibition of Complex III of the mitochondria be predicted by toxicodynamic and toxicokinetic NAM data?

The hypothesis is supported by mechanistic data, anchored to a putative AOP (based on the recently OECD adopted AOP on CI inhibition leading to parkinsonian disorder), and kinetic PBTK data. Thus, the following data was obtained: phys/chem, structural similarity, effects on oxygen consumption (mitochondrial complexes and whole cells), effects on mitochondrial membrane potential, cellular damage measured by effects on glycolysis and viability in three different cell types including neuronal cells, neuronal degeneration and neurite outgrowth.

The overall structural similarity of the compounds is less, however, they have the same pesticidal mode of action and toxophore.

Inhibition of CIII complexes measured by oxygen consumption, by the target compound azoxystrobin seemed to be slightly less strong than by the source compounds pyraclostrobin and picoxystrobin, while antimycin A resulted in a much stronger inhibition. This was confirmed with whole cells as well. Effects on membrane potential were marked by Antimycin A and orders of magnitude less with the target and source compounds. Effects on glycolysis and cell viability were similar between the compounds. The target compound was negative in the neurite outgrowth assay in SH-SY5Y cells, while some of the source compounds did show weak effects, and neither the target nor the source compounds were regarded as neurotoxic in the neuritetox assay in LUHMES cells.

The kinetic data and simulations confirm comparable kinetics and that the exposure of the brain to the strobilurins is limited being approx. twice the plasma concentration.

Overall, based on the generated data on kinetics and effect data, there is no evidence for a stronger neurotoxic potential of azoxystrobin mediated by a complex III inhibitory mode of action as compared to the source compounds. Since the source compounds do not show neurotoxicity *in vivo*, it is concluded that also the target compound azoxystrobin is not a neurotoxicant.

# *Table of Contents*

## Tables



## Figures

# 1. Introduction

Cellular respiration is an essential housekeeping process that yields large amounts of ATP. Cellular respiration depends on the functions of the membrane embedded protein complexes NADH dehydrogenase (CI), succinate dehydrogenase (CII), ubiquinol cyt *c* oxido reductase (CIII), cyt *c* oxidase (CIV) and ATP synthase (CV) (Figure 1.1) that are embedded in the mitochondrial inner membrane. In eukaryotic cells, these respiratory chain complexes are located in the inner mitochondrial membrane. These membrane protein complexes take part in the process of oxidative phosphorylation, where electrons from chemical reducing equivalents are transferred sequentially through a series of complexes, maintaining a proton motive force across the membrane for ATP synthesis.

The complex III (CIII) or $bc_1$ complex is the mid-segment of the respiratory chain. Structurally, it is a homo-dimeric complex, containing 10 to 11 subunits per monomer, of which only three subunits are essential for the electron transfer (ET) and proton translocation function: cyt *b*, cyt $c_1$ and the iron-sulphur-protein.

**Figure 1.1. Schematic representation of electron transport chain consisting of complex 1-V (OECD, 2018, Figure. 1)**

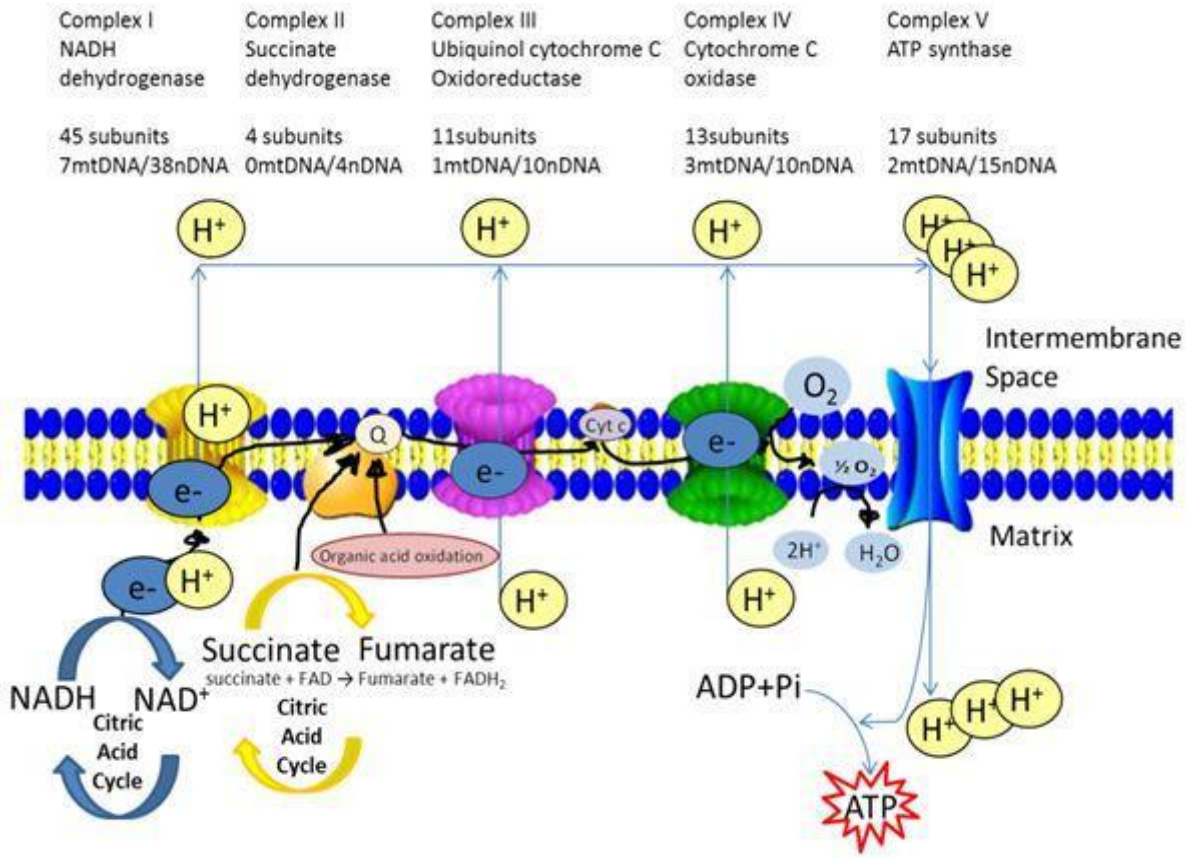

Inhibition of oxidative phosphorylation has evolved as an efficient strategy in nature to gain competitive advantage in survival and is used extensively in plant disease control. As a central component of the cellular respiratory chain, the CIII became an easy target for numerous natural antibiotics. Examples of natural compounds that specifically target CIII are antimycin from *Streptomyces* bacteria and strobilurin from *Strobilurus tenacellus* fungus.

The synthetic strobilurin fungicides are derived from the naturally occurring strobilurin A and B. The strobilurins bind to the quinol oxidation site of cytochrome *b* of CIII. This stops the electron transfer between cytochrome *b* and cytochrome *c* resulting in perturbed NADH oxidation and ATP production. The common chemical feature of the strobilurin is the (E)-β-methoxyacrylate group which is also considered to be the toxophore (Bartlett *et al.*, 2002).

There are ~10 different types of strobilurines registered as fungicides. When tested in standard regulatory mammalian toxicity studies they have been shown to be relatively safe, the critical effects being liver toxicity and decreased bodyweight. There are no signals of developmental and reproductive toxicity, nor carcinogenicity, except for one of the source compounds (kresoxim-methyl). As regards neurotoxicity, there are no strong signs from the standard repeat dose studies.

There are some signals of potential neurotoxicity from *in vitro* studies by a CIII-mediated mechanism. To date, there are no specific correlations found between fungicide, neither strobilurins, exposure and human health outcomes.

Some of the strobilurins have been tested in guideline compliant neurotoxicity (OECD TG 424) studies, and there was no sign of neurotoxicity.

The objective of this read-across case is to justify waiving of an OECD TG 424 study for azoxystrobin by means of NAM data.

# 2. Purpose

## 2.1. Purpose of use (targeted regulatory framework)

Currently, the European Pesticide regulation is undergoing a refit exercise and as part of this, several analyses have been carried out both regulatory/processual and scientifically on how the existing regulation is working and also providing recommendations on how the regulation could be improved. In this context the Chief Scientific Advisors of the Scientific Advice Mechanism, EU Commission DG Research and Innovation, based on an evidence review by the SAPEA (Science Advice Policy by the European Academies), published the report "EU Authorisation process of plant protection products - from a scientific point of view[1, 2]. The report calls for making better use of data and more specifically for bulk evaluations of groups of pesticides with the same pesticidal/toxic Mode of action to better enable read across between the pesticide active substances (SAPEA, 2018).

Although not comparable in terms of problem formulation, context and endpoint, there is an example of waiving of a study for a certain data requirement in context of pesticide regulation. The Office of Pesticide Programs (OPP), US EPA, accepted in the case of the active substance halauxifen-methyl the waiving of the chronic bioassay by bridging from a major metabolite of the parent. In this instance, mechanistic data was used in conjunction with PBPK modelling for justification (U.S. EPA, 2016).

On the other hand, *in vitro* data can trigger a concern which might need to be addressed by *in vivo* data as exemplified for neonicotinoid pesticides (EFSA, 2013).

**There are signals of potential neurotoxicity of strobilurins as *in vitro* data indicate a CIII-mediated mechanism (Pearson *et al.*, 2016, Regueiro *et al.*, 2015, Simon *et al.*, 2019). The purpose of this case study is to show that a neurotoxicity study (OECD TG 424) triggered by the potential neurotoxicity based on *in vitro* data would not be warranted based on other substances of the same class and their *in vivo* neurotoxicity data (OECD TG 424). There is no trigger from available OECD TG data. NAM data are used for the justification of this read across case.**

## 2.2. AOP framework

In this document, we want to provide support for a negative neurotoxicity prediction based on NAM data linked to a putative AOP. The putative AOP was compiled based on the previous approved AOP describing the relationship between mitochondrial complex inhibition in neuronal cells and the development of parkinsonian motor deficits (OECD, 2018a). The fundamental structure of the parkinsonian AOP is preserved, however the MIE is substituted for complex III inhibition and the AO for general neuronal toxicity (Figure 2.1). For all key events (except AO), a set of assays was selected to assess their perturbation upon exposure to strobilurins. Furthermore, the well-established complex III inhibitor

[1] Authorisation processes of plant protection products in Europe: http://ec.europa.eu/research/sam/index.cfm?pg=pesticides

[2] Europe's top science advisers send clear message on food production: https://www.nature.com/articles/d41586-018-05327-2

Antimycin A was included as a stressor with literature evidence supporting the proposed AOP flow.

**Figure 2.1. Putative AOP describing the relationship between complex III inhibition and neurotoxicity**

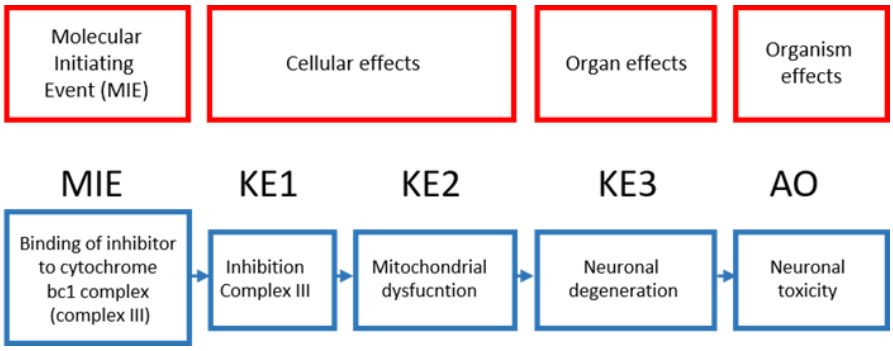


## 2.3. Complex III homology

Given the agricultural use of the source and target compounds and since the hypothesis is based on the assumption that CIII inhibition occurs in mammals as in fungi, a description of the homology is provided here.

Life depends on energy transduction mechanisms and therefore it is to be expected that the complexes of the electron transport chain (ETC) are extremely conserved in structure within species. Special consideration is given to ATP synthase and quinone - cytochrome c - oxidoreductase (CIII), which occur in mitochondria, prokaryotic plasma membranes, bacterial chromatophores, and chloroplast thylakoid membranes (Hatefi, 1985).

The atomic structure of CIII from a variety of organisms have been solved and show a high level of similarity within species (Xia *et al.*, 1997). The composition of all respiratory complexes in *H. sapiens* and *S. cerevisiae* they demonstrate highly similar, except for NADH-oxidoreductase (CI). CI is absent in S. cerevisiae and substituted by a type II NADH dehydrogenase (Figure 2.1), implicating a predominant role of complex III in yeast in maintaining the proton-driving force (Meunier *et al*, 2013).

Protein alignment of CIII of *S. cerevisiae* and *H. sapiens* shows 50% similarity (Figure 2.2). Protein BLAST analysis has shown high matches for residues that compose the catalytic core of complex III at the binding site for strobin inhibitors on $Q_o$, and on the respective haeme bH binding site, as well as on $Q_i$ and the respective haeme bL binding site (Figure 2.3 and Figure 2.4).

Comparison of the available crystal structures for CIII of yeast and vertebrates did not show features that would interfere with the coupling process of proton pumping and electron transfer of the Q-cycle mechanism (Berry, De Bari, & Huang, 2013).

The CIII crystal structure of yeast shows high similarity to the human enzyme, with 50 % identity for cyt *b*, making it possible to use yeast as a model to study genetic mitochondrial diseases associated with mutation in the cytochrome *c* gene MTCYB. Blakely had shown that the modelling in yeast of the human Arg318Pro mutation, causes severe deficiency in CI and CIII activities in a similar manner, suggesting the potential of using yeast as a model for mutation involving the cytochrome *b*. (Blakely *et al.*, 2005).

Finally, inhibition experiments with antimycin A ($Q_i$ site) and stigmatellin ($Q_o$ site) conducted in CIII of rabbit, cow and chicken have confirmed the conserved functionality of the pockets (Zhang, Yu, & Yu, 1998).

**Figure 2.2. Schematic representation of electron transport chain differences between mammalian and yeast (Meunier *et al.*, 2013)**

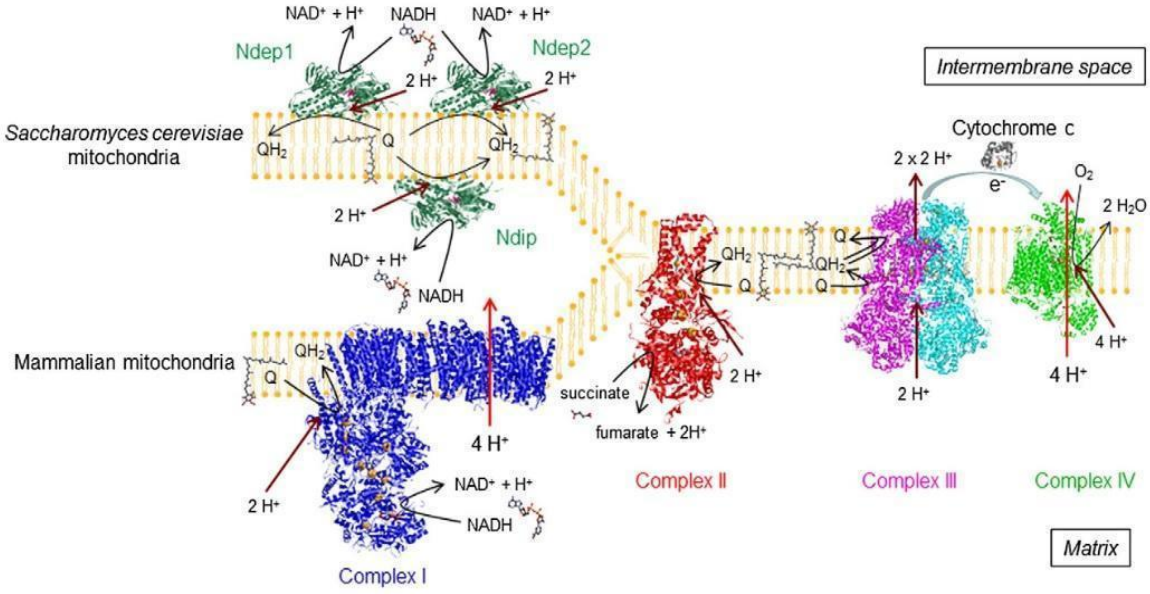


**Figure 2.3. Protein alignment of cytochrome *b* of *H. sapiens* (ACN37817.1) and *S. cerevisiae* (strain ATCC 204508 / S288c).**

The 50% similarity includes residues involved in the catalytic core of the complex.

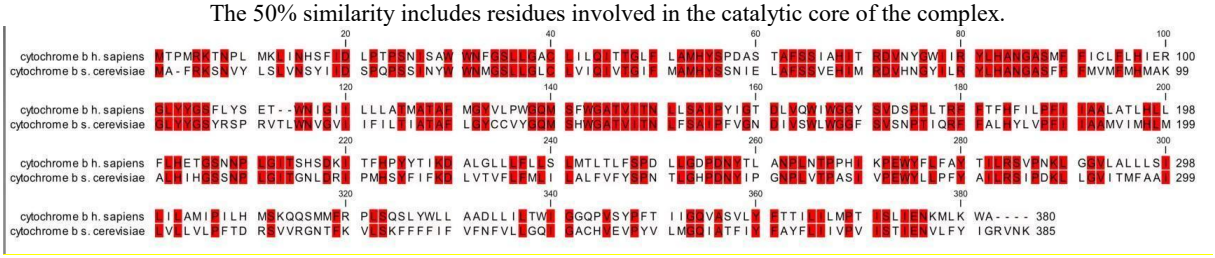


**Figure 2.4. Conserved domains in protein Blast analysis of *S. cerevisiae* (strain ATCC 204508 / S288c) cytochrome *b*.**

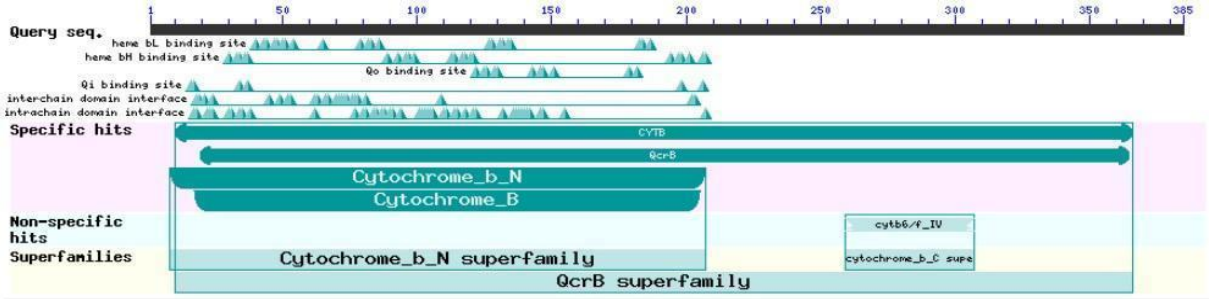

## 2.4. Target chemical(s)/category definition

Azoxystrobin is the target compound and is a member of the strobilurin family.

**Table 2.1. Chemical descriptors target compound**

| Compound | Azoxystrobin |
|---|---|
| Molecular Formula | C22H17N3O5 |
| Cas number | 131860-33-8 |
| Chemical structure | 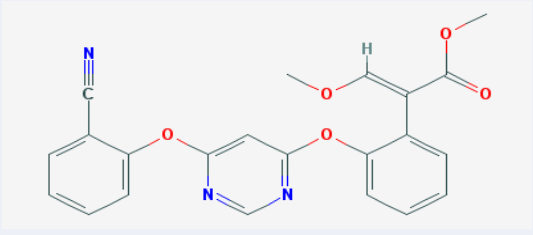 |
| MW | 403.394 g/mol |
| XLogP3-AA | 3.7 |

## 2.5. Endpoint(s) for which the read-across is performed

The endpoint for which the read-across is performed is low neurotoxic potential. Thus, the scientific **hypothesis** is: Can low neurotoxic potential of strobilurins, mediated by inhibition of mitochondrial complex III, be predicted by toxicodynamic and toxicokinetic NAM' data?

## 2.6. Exposure information

Not applicable for the read-across case described here.

# 3. Hypothesis for the analogue approach/category

The strobilurins bind to the quinol oxidation site of cytochrome b of complex III. This stops the electron transfer between cytochrome b and cytochrome c resulting in perturbed NADH oxidation and ATP production. The common chemical feature of the strobilurin is the (E)-β-methoxyacrylate group which is also considered to be the toxophore (Bartlett, 2002).

There are ~10 different types of strobilurines registered as fungicides. When tested in standard regulatory mammalian toxicity studies they have been shown to be relatively safe, the critical effects being liver toxicity and decreased bodyweight. There are no signals of developmental and reproductive toxicity, nor carcinogenicity. As regards neurotoxicity, there are no strong signals from the standard repeat dose studies, and according to the regulation EU 1107/2009 specific neurotoxicity testing becomes obligatory only if neurotoxicity has been observed during organ toxicity testing or in case of structural analogy with a known neurotoxic compound. However, clear and consistent criteria to trigger submission of such data are still lacking and for several of the compounds specific neurotoxicity studies have been conducted.

There are some signals of potential neurotoxicity of strobilurines from *in vitro* studies. For example, Regueiro *et al.* (2015) found that exposure to 0.1-100 µM for 7 days *in vitro* resulted in a dose-dependent toxicity in the MTT cell viability assay (measures metabolic activity of cells. MTT is the abbreviation of the dye compound; 3-(4,5-Dimethylthiazol-2-yl)-2,5-diphenyltetrazolium bromide) in primary cultured mouse cortical neurons. Kresoxim-methyl and pyraclostrobin were the most neurotoxic compounds (lethal concentration 50 were in the low micromolar and nanomolar levels, respectively) causing a rapid rise in intracellular calcium and strong depolarisation of mitochondrial membrane potential. Cell death was reversed by the calcium channels blockers MK-801 and verapamil, suggesting that calcium entry through NMDA receptors and voltage-operated calcium channels are involved in the neurotoxicity. The authors suggested a need for further evaluation of their neurotoxic effects *in vivo* (Regueiro *et al.*, 2015). Also, recently, Pearson *et al.* (2016) showed that several strobilurins, when tested in mouse neocortical neuron-enriched cultures, produced transcriptional changes similar to those seen in some cognitive and neurodegenerative diseases (Pearson *et al.*, 2016). The compounds disrupted microtubuli, mediated by free radical formation. Thus, there are some signals from *in vitro* studies that strobilurins could cause neurotoxicity by a CIII-mediated mechanism.

To date, there are no specific correlations found between fungicide (including strobilurins) exposure and human health outcomes. However, it must be acknowledged that epidemiological studies in regard to pesticide exposure have numerous shortcomings, not least the power of the studies (Ockleford *et al.*, 2017).

Some of the strobilurins have been tested in guideline compliant neurotoxicity (OECD TG 424) studies which have been assessed in Europe by the most recent draft assessment reports. In the studies described there were no signs of neurotoxicity.

The objective of this read-across case is to justify waiving of an OECD TG 424 study for azoxystrobin by means of NAM data. The formation of the category is based on the hypothesis that the compounds share similar chemical structure, similar pesticidal mode of action, similar toxophore, similar neurotoxic potential and similar toxicokinetics to azoxystrobin. Furthermore, compounds included in the category should have a

comprehensive toxicokinetic and toxicokinetic database and therefore only compounds assessed and approved in Europe are included in the category.

## 3.1. Chemical identity and composition

**Table 3.1. Chemical name and identity**

| Compound | Pyraclostrobin | Picoxystrobin | Trifloxystrobin | Kresoxim-methyl | Antimycin A |
|---|---|---|---|---|---|
| **Structure** | 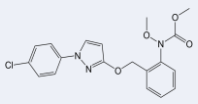 | 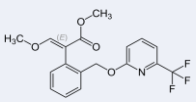 | 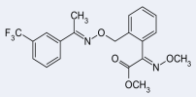 | 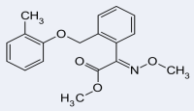 | 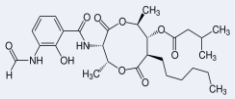 |
| **CAS number** | 175013-18-0 | 117428-22-5 | 141517-21-7 | 143390-89-0 | 1397-94-0 |
| **Molecular formula** | C19-H18-Cl-N3-O4 | C18-H16-F3-N-O4 | C20-H19-F3-N2-O4 | C18-H19-N-O4 | C28-H40-N2-O9 |

## 3.2. Physical-chemical properties and other molecular descriptors

The phys-chem properties of the source and target compounds are presented below in Table 3.2, Table 3.3 and Table 3.4.

**Table 3.2. Physical properties**

| Compounds | MW | H-bond donor | H-bond acceptor | LogP |
|---|---|---|---|---|
| Pyraclostrobin | 387.82 | 0 | 5 | 3.99 |
| Picoxystrobin | 367.324 | 0 | 8 | 3.99 |
| Trifloxystrobin | 408.377 | 0 | 9 | 4.5 |
| Kresoxim-methyl | 313.353 | 0 | 5 | 3.40 |
| Antimycin A | 548.633 | 3 | 9 | 4.75 |
| Azoxystrobin | 403.394 | 0 | 8 | 2.5 |

**Table 3.3. Chemical properties**

| Compounds | water solubility (mol/L) | | Vapour pressure (mmHg) | |
|---|---|---|---|---|
| | Experimental | predicted | Experimental | predicted |
| Pyraclostrobin | NA | 6.69e-5 | NA | 5.77e-9 |
| Picoxystrobin | NA | 2.96e-5 | NA | 8.27e-5 |
| Trifloxystrobin | NA | 4.56e-6 | NA | 3.15e-6 |
| Kresoxim-methyl | 6.38e-6 | 3.38e-5 | 1.72e-8 | 1.06e-6 |
| Antimycin A | NA | NA | NA | NA |
| Azoxystrobin | 1.49e-5 | 1.26e-5 | 8.25e-13 | 2.95e-11 |

Source = comptox EPA

**Table 3.4. Experimental chemical properties**

| Compounds | water solubility | Vapour pressure |
|---|---|---|
| Pyraclostrobin | 1.9mg/ml (at 20°C)[1] | 1.95*10-10 mm Hg (at 20°C)[1] |
| Picoxystrobin | 3.25 mg/ml (at 20°C)[6] | 0.0034 mPa (at 20°C) [7] |
| Trifloxystrobin | 0.610 mg/L (at 25°C) [2] | 2.55X10-8 mm Hg (at 25°C)[3] |
| Kresoxim-methyl | 2 mg/l (at 20°C)[4] | 1.72X10-8 mm Hg (at 20°C)[4] |
| Antimycin A | | |
| Azoxystrobin | 6 mg/L (at 20°C)[5] | 8.3X10-13 mm Hg (at 25°C)[5] |

Source = various

## 3.3. Kinetics: Absorption, distribution, metabolism and excretion

In all the studies described below the route of exposure was oral.

### *In vivo ADME*

The information described below, is a synthesis of information collected from EU Draft Assessment Reports. The level of detail and information available varies between the reports in particular quantitative information is very varied. This is partly explained by general heterogeneity in the data and the reporting of data and also because the compounds have been evaluated at different timepoints, thus reflecting the standards required at the time. It has not been possible to access the raw data.

### *Azoxystrobin (target compound):*

Results of radio-labelled studies in rats have shown that the absorption of the test compound is high, dose dependent and in excess of 80% at low doses. Biliary excretion was >70%, with >10% in the urine of non-cannulated animals. Excretion profiles were similar in both sexes and for different dose levels. In females, however, a somewhat lower biliary and slightly higher renal elimination than in males was observed although this difference was not very marked and was more pronounced following a low dose. Repeated administration of the low dose did not significantly alter the kinetic pattern. Absorbed azoxystrobin is well metabolised yielding at least 18 metabolites and rapidly eliminated with the bile being the main route. No parent compound was identified in the bile. In contrast, faeces contained predominantly unchanged azoxystrobin. The most abundant metabolite (V), representing approximately 25 - 30 % of the administered dose, is a glucuronide conjugate of azoxystrobin acid. Cleavage of the diphenyl ether links occurred to a very limited extent.

Tissue distribution:

Seven days after dosing (1 mg/kg - repeated dosing for 14 day), the rats were killed and the following organs and tissues were taken: brain, gonads, heart, large and small intestines, kidneys, liver, lungs, spleen and representative samples of blood for radiochemical analysis. Little radioactivity was retained in the tissues, with <0.8 % of the administered dose present in the tissues and carcass for either sex. The highest concentration of radioactivity was found in the kidneys.

### *Pyraclostrobin (source compound):*

The excretion balance of pyraclostrobin in rats demonstrated that only approximately 15% or even less of the applied radioactivity was excreted via the urine at 5 and 50 mg/kg bw.

Excretion via the faeces accounts for 80 – 90% of the dose. However, 35% of the dose was eliminated from the body via the bile. Summing up the amount of urinary and biliary excretion, bioavailability was estimated to be 50% or slightly less.

Oral absorption, although incomplete, is rapid and so is elimination. Initial half-lives are approximately 10 h, terminal half-lives range between 20 and 37 hours. AUC values of both dose levels suggest nearly linear kinetics. Elimination is nearly complete after 120 hours post dosing with the major part of radioactivity being excreted during the first 48 hours.

After oral administration to male and female rats, the systemically available portion of pyraclostrobin was rapidly and extensively metabolised to a large number of biotransformation products. N-demethoxylation was the quantitatively most important pathway. Phase I biotransformation is further characterised by various hydroxylations, cleavage of the ether bond and further oxidation of the two resulting molecule parts. Combinations of these reactions and the conjugation of the resulting OH-groups with glucuronic acid or sulphate led to a large number of observed metabolites.

Pyraclostrobin had a reduced serum cholinesterase activity in a 28 days study in rats at higher doses in females (roughly 47 and 126 mg/kg/day) but there was no effects on erythrocyte and brain cholinesterase. The NOAEL of the study was 9 mg/kg/day based on effects on body weight, haematological effects and liver effects. The Assessment Report suggest that the finding could be due to reduced synthesis of the esterase in the liver and not a direct.

Tissue distribution

Following the single high dose of $^{14}$C-pyraclostrobin, tissue radioactivity concentration was measured 0.5, 24, 36 and 72 hours after dosing. At dose level of 5 mg/kg bw, the corresponding radioactivity measurements were done at 0.5, 8, 20 and 42 hours after application. In general, tissue radioactivity levels in both sexes were in the same range at the respective time points and dose levels. The pattern of distribution and elimination in various organs and tissues was also similar. Throughout the time course of the experiments, by far the highest radioactivity concentrations were found in the GI tract in particular in stomach and stomach content. Among the other organs and tissues, highest values were found in the liver. Residues in most other organs and tissues were less than or similar to the plasma levels. Radioactivity concentrations were lowest in bone and brain. Due to the lipophilic properties of pyraclostrobin, residues in body fat were of particular interest. Towards the end of the observation period, radioactivity in adipose tissue clearly exceeded the plasma concentration. However, with the exception of low dose males, residues were lower than in the liver and a decline was apparent when the actual concentration after 72 or 42 hours was compared to the initial values.

### *Picoxystrobin (source compound):*

The oral absorption value was quantified in bile duct cannulated rats in the biotransformation studies. In a whole body autography (WBA) study, administration of either $^{14}$C-pyridinyl-picoxystrobin or $^{14}$C-phenyl-picoxystrobin demonstrated that there were no significant differences in routes of excretion or tissue distribution between the different radiolabelled forms.

Picoxystrobin was well absorbed (>75%) in rats following oral administration, with the greatest proportion of the systemic dose eliminated via bile and subsequently excreted in faeces. There were no significant differences in absorption, distribution and excretion

profiles of either between single low and high oral dose levels (10 and 100 mg/kg bodyweight) or between single and repeated oral doses (10 mg/kg bodyweight). There were no significant differences between the sexes in excretion and tissue distribution profiles.

In both sexes, excretion of administered radioactivity was both rapid and extensive, and predominantly in faeces. Over 120 hours, both males and females excreted mean totals of 99% and 96% of the administered radioactivity respectively. Urinary excretion mean totals were 21% and 34% for males and females respectively.

Picoxystrobin is extensively metabolised and 42 metabolites have been found, of which 34 have been structurally identified. The major route of metabolism was ester hydrolysis and glucuronide conjugation and was consistent following both single and repeated daily oral doses at 10 mg/kg body weight and following a single oral dose at 100 mg/kg body weight. This major route of metabolism was similar in males and females although there were some minor sex differences in metabolism.

Tissue distribution:

Studies showed that all tissue concentrations were low, however, brain distribution was not measured specifically but was just included in the carcass. With the exception of liver, kidneys, GI tract, blood and (in males only) bone, group mean tissue concentrations were less than 0.1mg equivalent picoxystrobin/g. The amount of administered radioactivity present in the tissue and residual carcass of males and females was 0.76% and 0.87%, respectively.

### *Trifloxystrobin (source compound):*

After oral administration of trifloxystrobin, the extent of absorption was influenced by the dose level and the sex of the animals. Female rats absorbed about 65% of the low dose (0.5 mg/kg bw) from the GI tract based on urinary and biliary excretion, and tissue residues, whereas in male rats the extent of absorption was only 56%. At the high dose (100 mg/kg bw), the absorbed portion decreased to about 55% and 45% of the dose in males and females, respectively. Furthermore, the AUC value increased only 130-times compared with a dose level ratio of 200:1.

Within 48 hours, 72 - 96% of the dose was eliminated with the urine and faeces independent of the dose level, pretreatment with non-radiolabelled trifloxystrobin, the site of label, and the sex of the animals. However, the routes of elimination were different in male and female rats. Within seven days, male rats eliminated approximately 15% of the dose via kidneys while females excreted 33% in the urine. Bile-duct cannulated rats demonstrate that the bile is the principal route of elimination of radioactivity in both males and females. There was evidence of the involvement of enterohepatic circulation in the excretion process.

The half-life times of the tissue residues after oral administration trifloxystrobin at a low and high dose, were very similar with either of the two labels demonstrating that the small amount of label-specific metabolites formed do not influence the overall depletion kinetics.

Trifloxystrobin was extensively metabolised at the low dose level (0.5 mg/kg) ca 5% unchanged parent in faeces, whereas at the high dose level (100 mg/kg bw) 31-47% unchanged parent was found in faeces.

Tissue distribution

After administration of trifloxystrobin maximal blood residues were found at 12 to 24 hours. Irrespective of the dose level and the sex of the animals, the residues in all tissues

depleted with half-life times of 14 - 40 hours, except blood and spleen of female rats dosed with the high dose (82 and 68 hours respectively).

Seven days after administration of trifloxystrobin at the low dose (0.5 mg/kg), the tissue residues were very low (total residues ≤0.5% of the administered dose). At the high dose, residues were about 126 and 108-fold higher than the low dose level, in males and females respectively. Some sex and label-specific differences in tissue residues were observed at the high dose level. Generally, tissue residues were higher in females than males. Label-specific differences were noted in the fat, kidneys, liver and plasma, but not in brain.

### *Kresoxim-methyl (source compound)*

After oral administration, Kresoxim-methyl showed a rapid but saturable and low absorption from the GI tract. Radioactivity was mainly excreted via faeces (66 to 81% of the dose) essentially as unchanged compound. The compound was rapidly and completely metabolised. The phase I biotransformation of the compound in rats comprised the cleavage of the ester, the oxime ether and the benzyl ether bonds, hydroxylation of ring A in para position to the existing oxygen substituent, and it subsequent oxidation to the corresponding carboxylic acid. The resulting OH-groups underwent conjugation with glucuronic acid or sulphate.

Due to saturable absorption, excretion after oral administration was mainly via faeces. There was no evidence of accumulation of radioactive material after repeated dosing.

Tissue distribution

Only small amounts of remaining radioactivity were found in the liver, organ/tissues, skin and carcass 120 h after dosing, suggesting that kresoxim-methyl does not accumulate. A quantitative whole-body autoradiography was conducted in which animals were sacrificed at 0.5, 2, 8, 24 and 96 h after a single oral administration. In both sexes, the fraction of absorbed compound was low and maximum concentration of radioactivity in tissues were obtained at 0.5 and 2 h after dose administration.

The highest levels of radioactivity were associated with the content of the gastro-intestinal tract, i.e. the organs of metabolism and elimination. Lower concentrations were found in liver and kidney with trace concentrations in the remaining tissues, namely blood, bone, bone marrow, brain, eyes, Harderian gland, lung, muscle, gonads, salivary glands, skin, thymus and thyroid.

Radioactive material was distributed in all tissues and organs throughout the body but 96 h after dosing concentration of radioactivity was less than 2% of the administered dose.

A summary of the data of the source compounds and the target compound is provided below.

**Table 3.5. Summary of ADME *in vivo* data**

| Compounds | Absorption | Distribution (brain) | Metabolism | Clearance |
|---|---|---|---|---|
| Azoxystrobin | High | Moderate | Extensive | High |
| Pyraclostrobin | Moderate | Moderate | Extensive | Moderate |
| Picoxystrobin | High | Not measured | Extensive | Extensive |
| Trifloxystrobin | Low | Low | Extensive | High |
| Kresoxim-methyl | Low | Low | Extensive | High |

### *Overall conclusion regarding in vivo exposure of the brain to strobilurines*

The available *in vivo* data in rats with exposures up to 2 weeks and at doses relevant for the general toxicity studies, also neurotoxicity, consistently show that there is little exposure to the whole brain compared to liver, kidney and blood of any of the tested strobilurins including azoxystrobin. However, these data do not have the granularity to address whether strobilurins might accumulate in specific parts of the brains. A caveat with this data is that these comparisons are based on the distribution of total radioactivity and do not indicate whether the parent chemical distributes into the brain. However, distribution to the brain would be less likely for metabolites that are more polar.

## 3.4. Mode/Mechanism of action or adverse outcome pathways (MOA/AOP); including experimental (NAM) data and *in silico* models – e.g. prediction of MIEs, key events

### *MoA*

The mitochondrial CIII is a trans-membrane enzyme that catalyses the transfer of electrons from ubiquinol to cytochrome c via the two quinone-binding sites $Q_o$ and $Q_i$ at the opposite sides of the membrane. This process is coupled to the translocation of protons across the inner mitochondrial membrane to contribute to the formation of the proton driving force needed for the ATP-synthase to drive the synthesis of ATP.

Three subunits form the catalytic core of the enzyme: the eight transmembrane helices cytochrome *b*, cytochrome $c_1$ and the iron-sulphur protein, and their assembly is fundamental for the correct functioning of Q-cycle (Blakely *et al.*, 2005).

### *AOP: Complex III inhibition leading to neurotoxicity*

The mechanistic understanding of the target/source compounds is based on the pesticidal mode of action being mitochondrial CIII inhibitors. Inhibition of the mitochondria of neuronal cells can cause adverse effects and in case of inhibition of CI leading to parkinsonian motor deficits, recently an AOP has been published by the OECD (OECD, 2018a). Partly building on the above OECD approved AOP, a putative AOP is outlined below to support the approach chosen for the testing strategy. The fundamental structure of the AOP on CI inhibition leading to parkinsonian motor deficits is preserved, however the MIE is substituted for complex III inhibition and the AO for neurotoxicity. Since CIII inhibition like CI inhibition perturb the function of the mitochondria it was assumed that this could also lead to neurotoxicity.

AOP = *Mitochondrial complex III inhibition leads to neuronal toxicity*

Stressor = *Antimycin A*

MIE = Binding of inhibitor to cytochrome bc1 complex (complexIII)

KE1 = Mitochondrial complex III inhibition

KE2 = Mitochondrial dysfunction

KE3 = Neuronal degeneration

AO = Neuronal toxicity

**Figure 3.1. Adverse outcome pathway on the inhibition of mitochondrial complex III leading to neurotoxic effects.**

A) Schematic representation of the MIE, KEs and AO belonging to the AOP and their organisation in different types of effects,

B) Table representing all assays discussed in this report that support the various key events of the AOP

A)

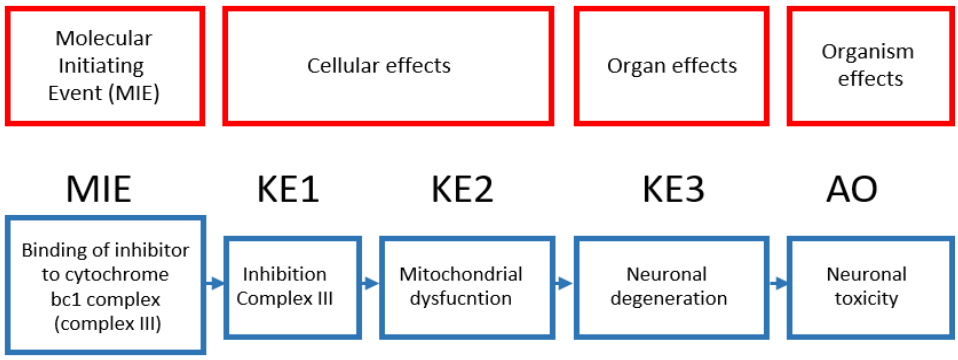


B)

| Key event | MIE | KE1 | KE2 | KE3 | AO |
|---|---|---|---|---|---|
| Assay | Receptor Docking studies | Seahorse assay (complex inhibition and whole cell) | Mitochondrial membrane potential assay | Viability assays (Resazurin, PI, ATP) | |
| | Similarity studies | | | Neuronal health (outgrowth and degradation) | |

In short, the proposed neurotoxicity AOP consists of 5 key events (KEs) from which one can be classified as adverse outcome (AO) at organism level and one as molecular initiation event (MIE).

**MIE: *Binding of inhibitor to cytochrome $bc_1$ complex*:** describes the physical allocation of a chemical the cytochrome $bc_1$ (complex III) binding pocket. Complex III of the electron transport chain, under normal conditions this enzyme catalyses the transfer of electrons from ubiquinol, reduced by complex I and II, to cytochrome *c* (25540143). The interaction between chemical and receptor can be assessed using docking studies in which both the study of chemical toxicophores of known ligands in combination with crystal structures of the receptor can provide information on the binding mode and binding efficiency of chemicals. Furthermore, similarity studies based on physchem parameters can provide insights into similarity of chemicals and the likelihood of similarity in binding modes.

**KE1: *Inhibition of cytochrome $bc_1$ complex*:** describes the interference of the inhibitor with complex III, which leads to a decrease, or total inhibition, of the reduction reactions needed to contribute to the generation of the proton gradient across the mitochondrial membrane. This proton motive force is used by the ATPase (CV) to produce ATP, prevention of CV activity leads to the total inhibition of oxidative phosphorylation (OXPHOS). To measure and quantify this key event, the seahorse bioanalyser can be used

to measure oxygen consumption rates (OCR) in permeabilised cells. The system is fed with specific substrates and inhibitors of the electron transport chain (ETC), allowing for determination of specific sites of inhibition along ETC.

**KE2: *Mitochondrial dysfunction*:** The drop in ATP production because of CIII inhibition and the lack of MMP will lead to total malfunctioning of mitochondria and stimulate the cell to switch to other sources of ATP production (like glycolysis). Changes in mitochondrial membrane potential (MMP) can be monitored with the use of specific fluorescent dyes. Probes as rho123 and JC-1 accumulates in healthy mitochondrial with a polarised membrane. Diminished or changed fluorescence reflect drops in membrane potential, due to electron transport chain inhibition.

When OXPHOS is inhibited as a consequence oxygen cannot be reduced to water at the level of complex IV. Changes in oxygen consumption rates (OCR) (mitochondrial respiration), can be measured *in vitro* using the Seahorse bioanalyser and reflect the level of inhibition of the target complex upon chemical exposure. Measurements of OCR in intact cells provide a physiologically relevant evaluation of direct effect of chemicals on mitochondrial respiration as well as information on the bioavailability of chemicals in cells.

Inhibition of OXPHOS will eventually lead to ATP depletion when the neurons cannot compensate the required ATP production through glycolysis. This can be measured as the intracellular ATP content after prolonged/repeated exposure by the luciferin/luciferase luminescence assay which is available as biochemical kits.

**KE3: *Neuronal degeneration*:** Lack of functional mitochondria will in the end lead to an overall drop in ATP levels in the cell, increase in production of reactive oxygen species (ROS), decreased neurite outgrowth, increased neurite degradation and eventually, stimulate the induction of cell death mechanisms. The subsequent observed effects upon neurons (reduced growth, degradation) can be visualised based on changes in morphological features of the cell, e.g. by quantifying neurite number and length in calcein-stained neurons after exposure to chemicals. Finally, the decreased viability that results from the drop in ATP can be followed using the resazurin to resorufin reduction reaction (a reaction dependent on the metabolic status of the cell). Another option is to assess the number of death cells using suitable cell death assays including propidium iodide staining of nuclei in necrotic cells.

**AO: *Neuronal toxicity*:** The prolonged induction of cell death will in the end manifest itself into neurotoxicity, e.g. neurodegenerative diseases.

### *Stressor for proposed AOP*

The AOP above is putative. In order to further develop the AOP, a way forward would be to look at the evidence of a suitable stressor compound. Experimental evidence supports for the chemical Antimycin A (a very well-described CIII inhibitor reference compound) that the previous cascade of events can lead to neurotoxicity. Below a list of studies demonstrating a relationship between Antimycin A and one or more of the previous described KEs.

#### *In vitro*

Antimycin A binds to the $Q_i$ centre of CIII, located to the negative side of the inner mitochondrial membrane, blocking the transfer of electrons from the haeme bH to ubiquinone. Antimycin A-induced inhibition of complex III of the electron transport chain has been shown to have severe effect in inhibiting the maintenance of mitochondrial

homeostasis in a large variety of tissues *in vitro*. Because of the specific mode of action, antimycin A has been used as an inducer of reactive oxygen species (ROS) production and oxidative stress in a vast number of *in vitro* studies, including nervous system models (Tokutake *et al.* 1994; Im *et al.*, 2013; Suh *et al.*, 2013).

Different studies have shown that antimycin A exposure is correlated with neurodegeneration *in vitro* via inhibition of oxidative phosphorylation. Zheng *et al.*(2016) addressed the treatment of mitochondrial related neurodegeneration, using antimycin A to induce impairment of oxidative phosphorylation in neurons derived from human embryonic stem cells and iPS neurons with inherent ATP synthase deficiency (T8993G). A set of inhibitors was used, including 1 µM antimycin A, for 6 h which resulted in high levels of lactate, pyruvate and amino acids, decreases in ATP and MMP as well as an increase in ROS production (Zheng *et al.*, 2016).

Pauwels *et al.* (1985) conducted a series of experiments to determine the effect of antimycin A, glucose and serum on cultured rat astrocytes, cerebellar neurons and mice neuroblastoma cells. They showed that the lack of glucose in the medium did not lead to a decrease in ATP production, while respiration blocked by treatment with antimycin A (1 µg/mg protein) led to a Pasteur effect, in which the cells increased the glycolytic rates to overcome the energy crises. When glucose supply was limited in the presence of antimycin A, the cells showed significant signs of degeneration such as loss of neurites, detachment from the substrate and release of LDH into the medium (Pauwels *et al.*, 1985).

There are contradictory studies about the direct link between mitochondrial dysfunction, i.e. mitochondrial depolarisation as a result of CIII inhibition, and mitophagy. Hytti *et al.*, (2019) showed that 25 µM Antimycin A induced cell death and mitophagy in retinal pigment epithelial cells. However, Shin *et al.* (2019) showed that 10 nM Antimycin A did not induce mitophagy in primary cultures of mouse neurons, although mitochondrial depolarisation took place. A third study showed that Antimycin A (10 ng/ml) had an inhibitory effect on autophagy (Ma *et al.*, 2011). One explanation to the contradictory results shown in the different studies may be due to the differences in concentrations of Antimycin A and that different cell types may respond differently to the compound. Nevertheless, mitophagy is not proposed as a KE in this AOP and may not be required for neurotoxicity.

In a study carried out by Bywood and Johnson (2003), rat brain slices were treated with different inhibitors of the electron transport chain to test different susceptibility between dopaminergic neurons in substantia nigra and hypothalamic neurons. It was shown that 2 h treatment with 20 µM antimycin A, lead to a severe decrease in ATP production, cell body damage with vacuolations and detachment from the surrounding neuropil and dendrite loss in dopaminergic neurons of substantia nigra. The pattern was found to reflect the damage of parkinsonian disorder brains post-mortem, whereas hypothalamic neurons were found more resistant showing no remarkable sign of damage. The two hypotheses for the differential degree of damage in the two neuronal types include the involvement of the excitotoxic mechanism, found implicated in many other degenerative disorders, or the increased susceptibility of the SN dopamine neurons to any insult compared to other types of neurons (Bywood and Johnson, 2003).

Lai *et al.* (2005) showed that antimycin A impaired the neuronal excitability in rat hippocampal CA1 slices. Furthermore, it was shown by patch clamp recordings that 3 µM antimycin A decreased the amplitude of persistent and transient sodium currents in hippocampal CA1 neurons. The attenuated currents were abolished by an inhibitor of

hydroxyl radical formation (PHEN), by MPG (a scavenger of $H_2O_2$) and stigmatellin (a $Q_o$ site inhibitor of complex III), implicating a role of ROS.

*In vivo*

There are no test guideline neurotoxicity studies found for antimycin A (PubMed, EPA.gov, echa.europa.eu). However, TOXNET displayed that adverse neurological effects like incoordination, impaired reflexes and CNS depression in animals, along with respiratory distress occur, but no references were given (https://toxnet.nlm.nih.gov/cgi-bin/sis/search2/f?./temp/~f4hJCs:3). Furthermore, neurodevelopmental defects in mouse embryos have been observed after a single s.c. injection of 3 mg/kg antimycin A. The neural tube defects were related to ROS formation and oxidative stress (Chang *et al.,* 2003).

*Complex III dysfunction and disease:*

The lack of direct evidence between antimycin A and neurotoxicity *in vivo* or in humans may be due to the potency of acute toxicity of the compound. As mentioned above, no accidental exposures of humans has been reported but acute exposure of animals indicate symptoms that suggest lethality by a neuronal mode of action. Further support for the suggested AOP are mutations in the CIII proteins leading to neurological dysfunction.

*Mutation studies*

Several studies show that mutations in genes encoding proteins that are necessary for cIII assembly or function are linked to progressive neurodegenerative disorders (Ghezzi *et al.*, 2011; Conboy *et al.*, 2018; Mordaunt *et al.*, 2015; Kunii *et al.*, 2015). Defects in tetratricopeptide 19 (TTC19) seem to be more represented, giving clinical AOs such as cerebellar ataxia, spastic paraparesis, sensory malfunction, epilepsy, developmental delay, absent reflexes and more (Mordaunt *et al.*, 2015; Kunii *et al.*, 2015; Ghezzi *et al.*, 2011). MRIs showed abnormal structures and necrotic lesions in caudate nuclei, substantia nigra, putamen (among other) (Ghezzi *et al.*, 2011). Studies of the mitochondrial activity in tissue samples from patients with defected TTC19 showed that cI and cII functions were normal, but cIII activity was attenuated (summarised by Mordaunt *et al.*, 2015).

In conclusion, the read across is relying on a putative AOP where CIII inhibition could lead to neurotoxicity. The AOP has been based on mechanistic data and sparse *in vivo* neurotoxicity data on Antimycin A and by the fact that CIII mutations can cause neurological impairments.

## 3.5. Responses found in alternative assays (e.g., experimental (NAM) data, *in silico*)

***Existing data on interaction of any of the strobilurin with CIII***

Strobilurins belong to class N inhibitors, which bind only in the $Q_o$ site of CIII (Berry & Huang, 2011). The binding-mode of the strobilurins will be described by means of azoxystrobin bound in the bovine crystal structure 1SQB. The methoxy methyl acrylate group of azoxystrobin is situated between Phe128 and Tyr313 and interacts with Glu271 via hydrogen bonding. The beta-methoxyacrylat stilbene blocks the access to the haeme. There are also hydrophobic interactions from the cyanophenoxyl moiety with Met124, Phe128, Ile146, Pro270, Phe274, Ala277, Leu294 and Ille298. Further on, the pyrimidyl

ring forms aromatic interactions with Phe128 and Pro270 (Esser, Scheffner, & Höhfeld, 2005) (Berry & Huang, 2011).

### ***In vitro data***

There are only few studies reported on strobilurin-induced toxicity using NAMs. Only four studies have been performed on neurons; two were performed using cultures of primary cortical neurons from embryonic mouse brain, one on N2a neuroblastoma cells and one on human neural stem cells. Other cell types used in NAMs are HepG2 liver cells (Shi *et al.*, 2017; Xia *et al.*, 2018), H9c2 cardiomyocytes (Rodrigues *et al.* 2015), L6 myocytes (Gao *et al.*, 2014), 3T3-L1 adipocytes (Gao *et al.*, 2014; Luz *et al.*, 2018), HaCaT keratinocytes (Jang *et al.* 2016) and cancer cell types (Shi *et al.,* 2017). Zebra fish larvae and *C. elegans* were used as other "non-animal" models. Studies on "wild life" organisms were not considered.

The literature search was performed in PubMed 13-14 September 2019, using the name of the strobilurins +cells or +neurons or +toxicity.

### *Mitochondrial dysfunction:*

Metabolic function and cellular fitness have been analysed by the resazurin reduction viability assay, mitochondrial membrane potential (by the TMRE fluorescence assay), and mitochondrial superoxide anion radical production by mitochondria using the MitoSOX fluorescent assay in the H9c2 rat cardiomyocyte cell line. The $IC_{50}$ values after 48 h of exposure with **azoxystrobin** in all endpoints were determined to approximately 1.2-1.5 mg/L (ca 2.9-3.7 µM) in average (Rodrigues *et al.*, 2015). Oxygen consumption (measured by a Clark-type oxygen electrode) was decreased in L6 myocytes and 3T3-L1 adipocytes after exposure with **azoxystrobin**, displaying $IC_{50}$ values of 0.63 µM and 0.31 µM, respectively (Gao *et al.*, 2014).

Cao *et al* (2018) found that mitochondrial complex III activity and ATP content were significantly decreased, ROS and lipid peroxidation (malone dialdehyde, MDA) production increased and oxidative stress mRNA markers were increased in zebra fish larvae after 8 days of exposure with 0.05 mg/L (124 nM) nominal concentration of **azoxystrobin** and in livers of adult zebra fish after exposure with 0.2 mg/L (496 nM).

Shi *et al.* (2017) reported $IC_{50}$ data on proliferation (measured by the MTT assay) in human cancer and non-cancer cell lines after exposure with **azoxystrobin**. Oesophageal Squamous Cell Carcinoma KYSE-150 cells showed reduced proliferation by 50% after 48h exposure with 2.42 mg/L (approximately 5 µM) and that this was correlated to cell cycle arrest and apoptosis. Other cell lines were less sensitive, e.g. $IC_{50}$ for HepG2 cells was 22.52 mg/L (Shi *et al.*, 2017).

Regueiro *et al.* (2015) showed in cultures of primary mouse cortical neurons that **pyraclostrobin** and **kresoxim-methyl** displayed highest toxicity of the compounds tested: $IC_{50}$ was 0.15 µM and 2.6 µM, respectively as analysed by the cell viability MTT assay after 24 hrs of exposure. The toxicity was mediated by an increase in the intracellular free $Ca^{2+}$ concentration (analysed by the Fluo-3 fluorescence assay) and mitochondrial membrane depolarisation (measured by Rhodamine 123 fluorescence). This study also shows the cellular uptake of the fungicides tested (Regueiro *et al.*, 2015).

Luz *et al.* (2018) showed that **pyraclostrobin** attenuated mitochondrial function in 3T3-L1 adipocytes and thereby, inhibited lipid homeostasis. MMP was analysed by JC-1, respiratory activity (e.g. oxygen consumption rate, steady-state ATP levels and

extracellular acidification rate) was monitored by the Seahorse set-up. 1 µM of pyraclostrobin decreased the ATP level by approximately 60% and increased ECAR by 100%, indicating a shift to glycolysis (Luz *et al.*, 2018).

Li *et al.* (2018) showed that **pyraclostrobin**, **trifloxystrobin** and **picoxystrobin** induced developmental toxicity and oxidative stress in zebra fish embryos at 96-h $LC_{50}$ values of 61, 55, 86 µg/L, respectively. Increased activity of ROS and MDA were observed as well as decreased activity of SOD and decreased levels of glutathione. Altered transcription of stress genes by the three strobilurins was observed by qPCR.

**Picoxystrobin** was identified as a mitochondrial toxicant compound in a tertiary screen using HepG2 and human neural stem cells (hNSC) within the ToxCast21 program. Intracellular ATP content (CellTiter Glo), MMP (JC-1), formation of ROS (ROS-Glo), upregulation of p53 and Nrf2/ARE (β-lactamase reporter assay, LiveBLAzer), mitochondrial oxygen consumption (Seahorse XF24) and cellular Parkin translocation (YFP-Parkin expression, confocal microscopy). Furthermore, larval development and ATP status were studied in the nematode *Caenorhabditis elegans* (Xia *et al.*, 2018).

Flampouri *et al.* (2018) investigated effects of **kresoxim-methyl** in murine neuroblastoma N2a cells. Exposure for 24h with 1 µg/ml (3.19 µM) reduced viability by 10% (neutral red uptake assay), increased mitochondrial ROS production (measured by MitoSOX Red/MitoTracker green), depolarised MMP by TMRE/MitoTracker Green, increased NO production ($NO^{2-}$ absorbance by the Greiss method) and attenuated migration by the scratch-induced wound closure method, but did not induce Caspase-3 activity (Ac-DEVD-pNA cleavage).

### *Mitochondrial dysfunction and autophagy:*

Jang *et al.* (2016) studied effects of **trifloxystrobin** on mitochondrial function and structure in human HaCaT keratinocytes. Cytotoxicity was determined after 48h of exposure by CCK-8 absorbance ($IC_{50}$ 3.32 µM) and 0.5 µM trifloxystrobin depolarised the mitochondrial membrane potential by >50% as shown by JC-1 (by flow cytometry, red/green ratio) and MitoTracker Red CMXRos (by confocal fluorescence microscopy). Autophagy was confirmed by immunofluorescence and western blot detecting increased expression of autophagy markers after 48h exposure with 0.5 µM trifloxystrobin. Increased mitophagy was detected after exposure with 0.5 µM trifloxystrobin by Cyto_ID Autophagy detection kit (Enzo Life Sciences) and increased expression of PINK and Parkin. Trifloxystrobin-induced mitophagy was abolished by the mROS scavenger mitoTEMPO.

### *Adverse outcome: Neurotoxicity*

**Pyraclostrobin** (0.1 µM) and **trifloxystrobin** (10 µM) were clustered in a group of compounds that altered gene expression in differentiating cultures of primary mouse cortical neurons in a similar fashion as found in pathologies such as the aging brain, autism spectrum disorders and Huntington's disease, but not in Parkinson's disease. Azoxystrobin (0.1 µM) was not clustered in any group of chemicals that correlated to neurodegenerative or neurodevelopmental diseases (Pearson *et al.*, 2016).

## 3.6. Information obtained from other endpoints/species/routes

**Effects on the nervous system (*in vivo*)**

The data below where collated from the most recent EU draft assessment reports.

**Pyraclostrobin:** Pyraclostrobin was tested in an acute (single dose of 0, 100, 300 and 1000 mg/kg bw - NOAEL was the highest dose tested) and in a short-term (0, 50, 250 and 750 (males only) or 1500 ppm (females) for 3 months - NOAEL was the highest dose tested)) neurotoxicity study in rats. These studies included extensive functional observation batteries as well as neuro-histopathological investigations. No indications of a specific neurotoxic potential of pyraclostrobin were observed confirming the lack of toxic properties of this kind as suggested by the other toxicological studies.

**Picoxystrobin:** There are no specific neurotoxicity studies with picoxystrobin. In the mandatory repeat dose studies, there were no signs of neurotoxicity.

**Trifloxystrobin:** Rats given a single oral dose of trifloxystrobin at 2000 mg/kg bw did not show effects indicating that trifloxystrobin is not neurotoxic. The neurotoxic potential of trifloxystrobin was also investigated as part of a 90 day dietary study in the rat. The following doses were administered 100, 500, 2000 and 8000 ppm via food. The functional observational battery (FOB) revealed no indications for a potential neurologic or behavioural effect of trifloxystrobin. No changes of toxicological relevance were observed in any of the parameters associated with motor activity. Neuropathological examination of tissues of the central and peripheral nervous system did not reveal any treatment-related neuropathic changes.

**Kresoxim-methyl:** In an acute neurotoxicity study compliant with OPPTS 870.6200 of US EPA kresoxim-methyl showed no sign of neurotoxicity up to a dose of 2000 mg/kg. In a 90 day repeat dose study rats were exposed to 0, 1000, 4000 or 16000 ppm. There were no signs of neurotoxicity and the NOAEL was 16000 ppm (~1180 mg(kg/day).

A summary of the *in vivo* neurotoxicity data is provided in the table below.

**Table 3.6. Summary of neurotoxicity *in vivo* data**

| Compounds | Dose (mg/kg) | study | NOAEL (mg/kg) |
|---|---|---|---|
| Pyraclostrobin | 0, 100, 300, 1000<br>0, 4, 20, 50, 112 | Acute<br>90-days | 1000<br>112 |
| Picoxystrobin | none | none | none |
| Trifloxystrobin | 0, 2000<br>0, 7, 33, 133, 620 | Acute<br>90-days | 2000<br>620 |
| Kresoxim-methyl | 0, 2000<br>0, 84, 341, 1354 | Acute<br>90-days | 2000<br>1354 |

## 3.7. Information on fate in the environment (hydrolysis, biodegradation)

Not Applicable.

## 3.8. The route and duration of expected exposure.

See above in description of existing *in vivo* data.

# 4. Source chemicals/Category members

## 4.1. Identification and selection of source chemicals/category members

The category members considered for the purpose of this read across were other pesticidal active substances pyraclostrobin, picoxystrobin, trifloxystrobin and kresoxim-methyl with a similar pesticidal mode of action, i.e. inhibition of mitochondrial CIII of fungi. The common chemical feature of the strobilurins is the (E)-β-methoxyacrylate group, Figure 4.1.

**Figure 4.1. Structure of the natural parent compounds of the strobilurins, strobilurin A.**

The red circle marks the (E)-β-methoxyacrylate group.

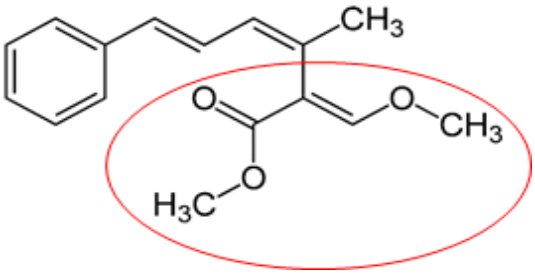


Since some *in vitro* data indicate that the compounds may have neurotoxic potential by a CIII-mediated mechanism, the purpose of the read-across was to establish that the target compound (azoxystrobin) is *not* neurotoxic by this mechanism as established for the source compounds.

Since the purpose is to characterise the potential CIII-mediated neurotoxicity of azoxystrobin by read-across to *in vivo* neurotoxicity data of other strobilurins, and to ensure a robust database, only strobilurins that had undergone an European evaluation and approval were selected. There is robust data for the particular endpoint (accepted regulatory studies, i.e. TG 424 complaint studies for several of them) and also supporting evidence from repeat-dose studies (28/90 days studies and chronic studies). The studies conducted of relevance for the endpoint are further supported by toxicokinetic data in rat.

Antimycin A is not used strictly as a source compound (the structure/phys/chem/toxicity is significantly different from the strobilurins) but since the hypothesis is to predict low neurotoxicity of the target, antimycin A is included as a "reference", since it is a mitochondria complex III inhibitor that is neurotoxic.

List of source chemicals/category members (including chemical identifiers)

**Table 4.1. Chemical name and identity**

| **Compound** | Pyraclostrobin | Picoxystrobin | Trifloxystrobin | Kresoxim-methyl | Antimycin A |
|---|---|---|---|---|---|
| **Structure** | 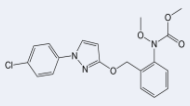 | 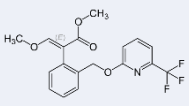 | 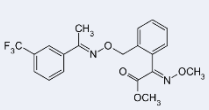 | 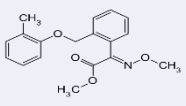 | 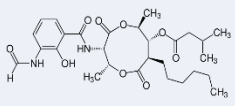 |
| **CAS number** | 175013-18-0 | 117428-22-5 | 141517-21-7 | 143390-89-0 | 1397-94-0 |
| **Molecular formula** | C19-H18-Cl-N3-O4 | C18-H16-F3-N-O4 | C20-H19-F3-N2-O4 | C18-H19-N-O4 | C28-H40-N2-O9 |

# 5. Data gap filling and Justification

## 5.1. Data gathering

For our AOP-based testing strategy, we have selected a panel of *in silico* and *in vitro* test methods. Neurotoxicity is per definition any process which adversely affects physiological neuronal structures or function. *In vivo*, this can be measured by behavioural analyses or histology. *In vitro*, there is a debate, whether "adversity" can be assessed directly. Instead, the concept of AOP is applied to link mechanistic (so-called intermediate) steps to adverse outcomes. Following this logic (Leist *et al.*, 2017, Terron *et al.*, 2018; OECD 2018b), assays for the MIE (receptor docking & similarity studies), KE1 (Seahorse respiration assays on permeabilised cells for individual mitochondrial complex analysis and on intact cells for total cellular affection of oxygen consumption) and KE2 (mitochondrial membrane potential assay) are used to investigate whether there might be a molecular cause for neurotoxicity. Furthermore, the assays applied for KE3 (viability assays and neurodegeneration/neurite outgrowth assays) are closely related to the human AO as they directly assess neuronal integrity. In earlier publications, it has been shown that specifically neurotoxic substances can be identified by the neurite outgrowth assay (Stiegler *et al.*, 2011, Krug *et al.*, 2013,). Below we briefly describe these test systems. More details descriptions for the various test systems can be found in the annex.

### *MIE: interaction with complex III*

To improve understanding of chemical properties and the associated target binding properties of the tested chemicals, we performed both a structure similarity study and a docking study.

1. *Chemical similarity assessment*

   The similarity of the chemicals has been addressed on 3 levels: Tanimoto coefficient, 3D structural similarity and SMART similarity

2. *Binding mode of complex III inhibitors*

   We have used structure based modelling to evaluate the chemical-target interaction. This method provides information on the likelihood of chemical-interaction with specific binding sides in complex III.

### *KE 1: complex III inhibition*

1. *Effects on oxygen consumption (isolated complexes)*

   For measurement of complex III activity, we used the Seahorse instrument. This instrument can determine the activity of different mitochondrial respiratory complexes. The activity is based on the oxygen consumption rate using permeabilised cells and the application of specific substrates for complex III. The Seahorse instrument is the gold-standard commercial available instrument that is used in labs worldwide to determine mitochondrial respiratory chain complex activity. The activity of complex III was determined in the neuronal LUHMES cell line that represents dopaminergic neurons.

### *KE2: mitochondrial dysfunction*

1. *Effects on oxygen consumption (whole cells)*

   The Seahorse instrument was used to determine the oxygen consumption mediated by the respiratory chain. In this case, intact non-permeabilised cells were used in the assay. We used three different test systems: neuronal LUHMES cells, renal RPTEC, and liver hepatoma HepG2 cells; all test systems have functional mitochondria.

2. *Effects on mitochondrial membrane potential*

   When complex III of the mitochondrial respiratory chain is blocked the mitochondria cannot establish a mitochondrial membrane potential. Therefore, assessment of the mitochondrial membrane potential is another mean to assess dysfunction of the mitochondria. For this, we have used a high content imaging setup making advantage of fluorescent dyes that accumulate in the mitochondria based on the existence of the membrane potential. The amount of fluorescent dye is dependent on the mitochondrial membrane potential. Using microscopy, the levels of the fluorescent dye can be visualised and quantified in individual cells. We have analysed the effect on the mitochondrial membrane potential in two test systems: HepG2 and the neuronal SH-SY5Y dopaminergic neuron cell line.

3. *Effects on glycolysis*

   As a consequence of perturbation of the mitochondrial respiration, cells will switch their ATP production to the oxygen independent glycolysis. A measure of for this switch is the increase of a glycolysis by-product lactate. The lactate levels were measured in HepG2, RPTEC and SH-SY5Y cells.

4. *ATP levels*

   As a consequence of mitochondrial dysfunction, cells cannot produce ATP through the flux of protons through the F0F1ATPase (complex V) of the mitochondria. An indirect measure of mitochondrial dysfunction is therefore the loss of ATP in cells. Intracellular ATP levels were monitored in SH-SY5Y dopaminergic neurons after 120 hr (repeated) exposure.

### *KE3: neuronal degeneration*

1. *Effects on cell viability*

   The decrease of cell number/ cell viability which is associated with neuronal degeneration can be assessed based on various viability measurements. The viability measurement used in this report is resazurin reduction and for SH-SY5Y neuronal cells, also relative number of cells with no propidium iodide (PI) staining of necrotic cell nuclei. Healthy cell are able to convert the colourless substance resorufin into the purple coloured resazurin. A loss of viable cells and a loss of viability per cell will lead to a decreased resazurin reduction. The associated colorimetric change can be used as measure for viability of the *in vitro* system.

2. *Effects on neurite outgrowth*

   For the degeneration of dopaminergic DA neurons, we have used assays that report on the phenotypic organisation of DA neurons. This is based on the loss of neurites that can be identified in DA neuron cultures. This assay is based on live cell

imaging where cultured neuronal cells are stained with calcein-AM, allowing the visualisation of cell bodies and neurites that are extending from the cell body. Image analysis allows the quantification of the neurite outgrowth. Loss of these neurites is representative for degeneration of DA neurons. These assays are performed with LUHMES and SH-SY5Y neuronal test systems.

### *Repeat dosing*

To assess the effects of prolonged chemical-exposure, LUHMES, SH-SY5Y and RPTEC/TERT1 were exposed repeatedly to the test chemicals. Various readouts were used to study the effects on the *in vitro* cell system

1. Repeat dose toxicity (LUHMES): Neurite outgrowth and viability
2. Repeat dose toxicity (SH-SY5Y): ATP content, neurite degeneration and viability (PI staining)
3. Repeat dose toxicity (RPTEC/TERT1): Lactate concentration and resazurin

### *In vitro in silico model (bioavailability)*

To allow a proper evaluation of the cellular concentrations of the strobilurin compounds, we have used a computational approach to model the intracellular concentrations. The model was verified by measuring the cellular and medium concentration of azoxystrobin using bioanalytical methods. These *in vitro* bioavailability predictions are required for a quantitative *in vitro* to *in vivo* extrapolation of our *in vitro* data on the KE activation measurements.

### *PBPK*

We used physiology-based pharmacokinetic (PBPK) modelling to predict the human tissue concentration and the *in vivo* rat concentration upon exposure to the test compounds. The methodology for PBPK modelling have been based on the approaches outlined in the WHO guidelines and detailed descriptions can be found in the annex.

**MIE: interaction strobilurin with the mitochondrial complex III.**

## *1. Chemical Similarity*

### Assessment of structural similarity

Structural similarity was calculated by using a workflow integrated into a KNIME analytic platform[3]. We used smiles codes as input parameter.

Smiles codes were extracted from high quality open source databases. In this case, the majority comes from the US EPA chemical dashboard[4] and one from CHEMID Plus[5] (Table 5.1). Prior to the calculation of structural fingerprints, the smiles codes for all analogues were quality controlled, a correction was not needed.

We used a fingerprint method, which involves encoding the structural information within a molecule as a bit string in which each bit indicates the presence of ("1") or absence ("0")

[3] KNIME Software: https://www.knime.com/knime-software
[4] US EPA chemical dashboard: https://comptox.epa.gov/dashboard
[5]ChemIDplus: https://chem.nlm.nih.gov/chemidplus/

of a particular molecular feature. Molecular fingerprints per compound were calculated with RDKIT using a MACCS keys (Molecular ACCess System). MACCS keys (Durant JL *et al.* 2002) are a classical fingerprint in chemoinformatics consisting of a dictionary of 166 structural fragments, as well as UNITY fingerprints (Patterson DE *et al.,* 1996) that assemble atom pathways of pre-defined lengths.

In order to assess structural similarity between compounds we used the Tanimoto coefficient. The Tanimoto coefficient (S) calculates similarity comparing pairs of compounds, e.g. A and B (Equation 1). It uses three values, the number of bits set to 1 in both fingerprints (value a and b) and the number of shared bits set to 1 between the two compounds (value c, equation 1).

$$\text{Equation 1: } S(A, B) = \frac{c}{(a + b - c)}$$

**Table 5.1. Chemical name and identity**

| name | SMILES | MW | Structure source |
|---|---|---|---|
| Azoxystrobin | CO/C='C('/C(=O)OC)c1ccccc1Oc1cc(Oc2ccccc2C#N)ncn1 | 403,394 | EPA |
| Pyraclostrobin | COC(=O)N(OC)c1ccccc1COc1ccn(-c2ccc(Cl)cc2)n1 | 387,823 | EPA |
| Picoxystrobin | CO/C='C('/C(=O)OC)c1ccccc1COc1cccc(C(F)(F)F)n1 | 367,323 | EPA |
| Trifloxystrobin | CO/N='C('/C(=O)OC)c1ccccc1CON=C(C)c1cccc(C(F)(F)F)c1 | 408,376 | EPA |
| Kresoxim-methyl | CO/N='C('/C(=O)OC)c1ccccc1COc1ccccc1C | 313,353 | EPA |
| Antimycin A | CCCCCC[C@H]1C(=O)O[C@H](C)[C@H](NC(=O)c2cccc(NC=O)c2O)C(=O)O[C@@H](C)[C@@H]1OC(=O)CC(C)C | 548,633 | ChemIDplus |

Structural similarity has been determined by the Tanimoto coefficient. The results are presented below in Table 5.2.

**Table 5.2. Tanimoto coefficients**

| name | Tanimoto Coefficient *S* |
|---|---|
| Pyraclostrobin | 0,52 |
| Picoxystrobin | 0.3 |
| Trifloxystrobin | 0.69 |
| Kresoxim-methyl | 0,53 |
| Antimycin A | 0.56 |

Two structures are usually considered structurally similar if S>0,85. The strobilurines source compounds show tanimoto scores well below this threshold when compared to the target compound azoxystrobin. This reflects the structural variation in those parts of the molecule, which are not relevant for the pesticidal and toxicological mode of action. However, the moiety representing the toxophore is structurally identical in all molecules, apart from antimycin A. Consequently, the Tanimoto coefficient does correctly characterise the structural features of the whole molecule, however, does not reflect the similarity in bioactivity. It has to be noted, that the structural variation in the molecules could have an impact on their toxicokinetic behaviour.

In cases like the present, where the mechanism of action depends on the specific interaction of the compounds with a defined protein binding site (mitochondrial complex III), the 3D properties of the compound structure play a major role. Therefore, molecular descriptors able to characterise the 3D shape can have advantages over 2D descriptors (like the aforementioned MACCs molecular fingerprints)

3D shape descriptors with atom types USR-CAT (Schreyer & Blundell, 2012) were calculated using 10 conformers obtained from RDKit[6]. Results are shown in the below heatmap and table.

**Figure 5.1. 3D Similarity matrix**

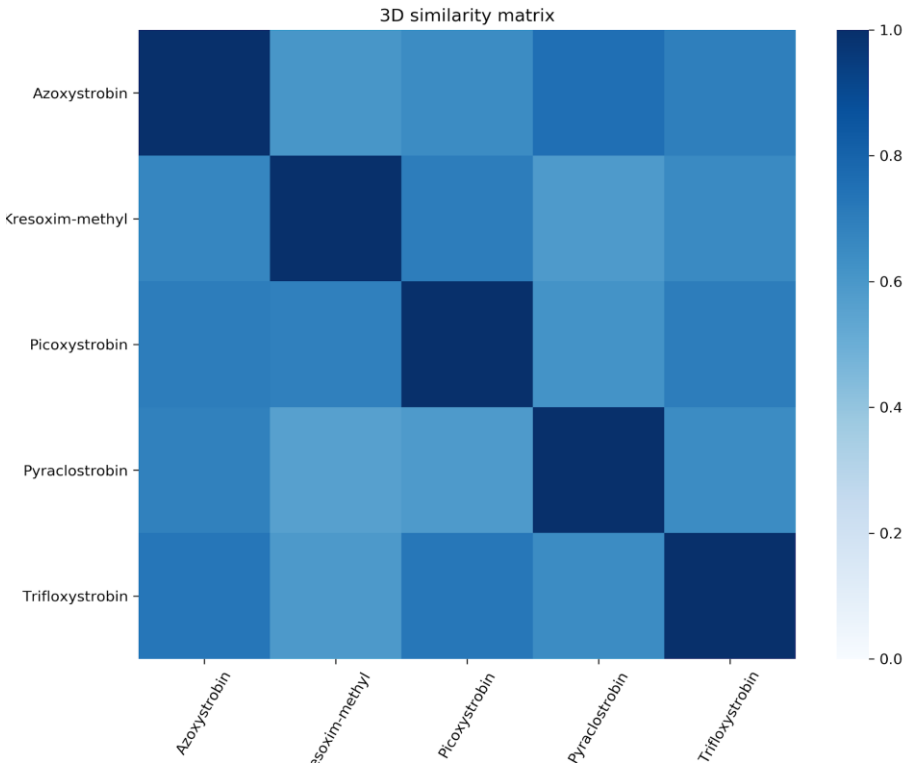


**Table 5.3. 3D similarity**

| | Azoxystrobin | Kresoxim-methyl | Picoxystrobin | Pyraclostrobin | Trifloxystrobin |
|---|---|---|---|---|---|
| Azoxystrobin | 1 | 0.61 | 0.65 | 0.76 | 0.7 |
| Kresoxim-methyl | 0.67 | 1 | 0.71 | 0.59 | 0.65 |
| Picoxystrobin | 0.7 | 0.69 | 1 | 0.62 | 0.7 |
| Pyraclostrobin | 0.69 | 0.56 | 0.59 | 1 | 0.64 |
| Trifloxystrobin | 0.73 | 0.59 | 0.72 | 0.65 | 1 |

It must be noted that the use of this 3D descriptors represents better the internal similarity of the compounds of interest with values ranging 0.61-0.76 for Azoxystrobin (compared with the 2D similarity ranging 0.3-0.69)

A different strategy to characterise the compound similarity is the use of SMARTS patterns (*SMARTS - A Language for Describing Molecular Patterns*[7], which overcomes some of the limitations of using Tanimoto and molecular fingerprints similarity. SMARTS search

[6] RDKit: Open-Source Cheminformatics Software: http://www.rdkit.org

[7] SMARTS - A Language for Describing Molecular Patterns: http://www.daylight.com/dayhtml/doc/theory/theory.smarts.html

returns only compounds having the same structural patterns. Three SMARTS patterns, matching all the compounds of interests have been defined, as it is shown in the table below:

**Table 5.4. SMART similarities**

| | SMARTS | | |
|---|---|---|---|
| **Compound** | C-O-[C,N]=C(-c:1:c:c:c:c:c:1)-C(=O)-O-C | C-O-N(-c:1:c:c:c:c:c:1)-C(=O)-O-C | O-C(=O)-C(-C(=C-C=C-c:1c:c:c:c:c:1)-C)=C-O-C |
| **Azoxystrobin** | | | |
| **Picoxystrobin** | | | |
| **Kresoxim-methyl** | | | |
| **Trifloxystrobin** | | | |
| **Pyraclostrobin** | | | |
| **Strobilurins (A…)** | | | |

Although, the structural similarity between the target and source compounds is low, based on the above, it is concluded that the target and the source compounds have similar structures as they share the methoxyacrylate moiety and have a similar 3D-shape that characterises better the category than 2D similarity.

Further information about these SMARTS and a comparison with Tanimoto/fingerprints similarity metrics is included in the Annex.

## *2. Binding mode of complex III inhibitors*

In CIII two known binding pockets exist, the $Q_o$ and the $Q_i$ site. Crystal structures with bound inhibitors have been published, amongst others, of the bovine and the chicken CIII. The strobilurins bind in the $Q_o$ site (Esser *et al*., 2004; Berry & Huang, 2011), whereas antimycin A is an inhibitor of the $Q_i$ site. The main interactions for antimycin A are the hydrogen bonds between Asp228 and a water molecule. The water molecule additionally interacts with Lys227 and Ser35 (Huang, Cobessi, Tung, & Berry, 2005).

For modelling complex III, the human cryo-EM structure 5XTE has been used. Molecular docking of antimycin A was performed into the human crystal structure of CIII by using Schrödinger[8]. The pocket was superimposed with the bovine crystal structure beforehand. Our methodology could reproduce a similar binding orientation in the human species, Figure 5.2.

[8] Schrödinger: https://www.schrodinger.com/

**Figure 5.2. Docking of Antimycin A into Complex III: binding mode of Antimycin A in bovine CIII could be partly reproduced for human CIII.**

Pink: docked antimycin A in human CIII; Yellow: antimycin A crystallised in bovine CIII

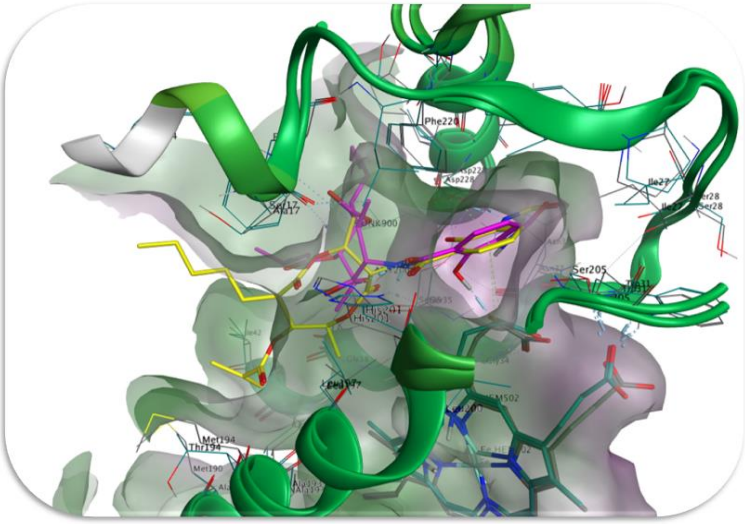


## *KE 1: complex III inhibition*

### *1. Effects on oxygen consumption (complexes)*

The quantification of the MIE, inhibition of mitochondrial respiratory chain (MRC) CIII, was performed by permeabilised LUHMES cells and subsequent sequential direct feeding of their MRC complexes. For both, the two tested source compounds pyraclostrobin and picoxystrobin (50 µM final concentration) a strong CIII inhibition (>80% of control) could be observed, whereas for the target compound azoxystrobin (50 µM final concentration) the inhibition was >50% of control. Observed inhibition of complex I and II in the three cases is consistent with their functional link with CIII, i.e. complexes I and II appeared to be inhibited since they cannot deliver their products to CIII anymore. Since complex I and II inhibition was observed to be comparable to the CIII inhibition, only CIII inhibition can be assumed. Inhibition of CIII by the target compound azoxystrobin seemed to be slightly less potent than by the source compounds pyraclo- and picoxystrobin, while antimycin A resulted in a stronger inhibition.

**Figure 5.3. Assessment of single mitochondrial respiratory chain complex inhibition.**

Proliferating LUHMES cells were plates into Seahorse culture plates and allowed to grow until 90% confluency. Then the cells were permeabilised with digitonin and fed sequentially with substrates for complex I to IV while the respective upstream complex was inhibited. The substance of interest (dissolved in 0.1% DMSO final concentration) was injected prior to the substrates. Inhibition was quantified relative to DMSO control samples. For both, the two tested source compounds pyraclostrobin and picoxystrobin (50 and 50 µM final concentration, respectively) a strong complex III inhibition (>80% of control) could be observed, whereas for the target compound azoxystrobin (50 µM final concentration) the inhibition was >50% of control. Antimycin A (50 µM) inhibited cIII activity to >88%. Observed inhibition of complex I and II in the three cases is consistent with their functional link with complex III.

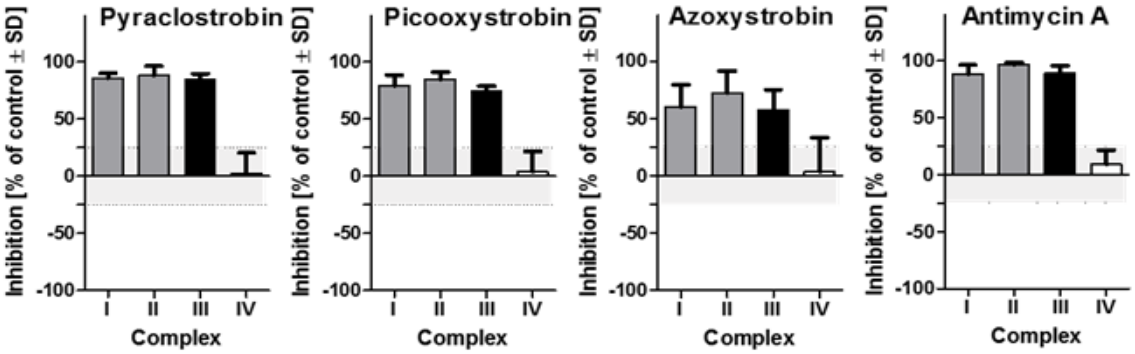


## *KE2: mitochondrial dysfunction*

### *1. Effects on oxygen consumption (whole cells)*

To investigate the effect of the compounds not only on individual MRC complexes, but also on key parameters of mitochondrial function, oxygen consumption rates (OCRs) were measured directly before and after treatment of whole cells using a Seahorse analyser.

**Figure 5.4. Assessment of mitochondrial dysfunction of intact cells through quantification of oxygen consumption of intact cells.**

Top) LUHMES cells on day 3 of differentiation (day of the endpoint quantification of the neurite outgrowth assay). An acute injection of a high, non-cytotoxic concentration (antimycin a, azoxystrobin, picoxystrobin 50 µM, kresoxim-methyl 12.5 µM, pyraclostrobin and trifloxystrobin 20 µM) completely inhibited cellular mitochondrial oxygen consumption. Except from azoxystrobin- and kresoxim-methyl, where a minor respiration was still detectable after 50 min treatment. All tested cIII inhibitors inhibited mitochondrial oxygen consumption directly and maximally.

Bottom) Differentiated RPTEC/TERT1 cells were injected with 10 µM of test compound, oxygen consumption rates were measured for 20 minutes before and after injection.

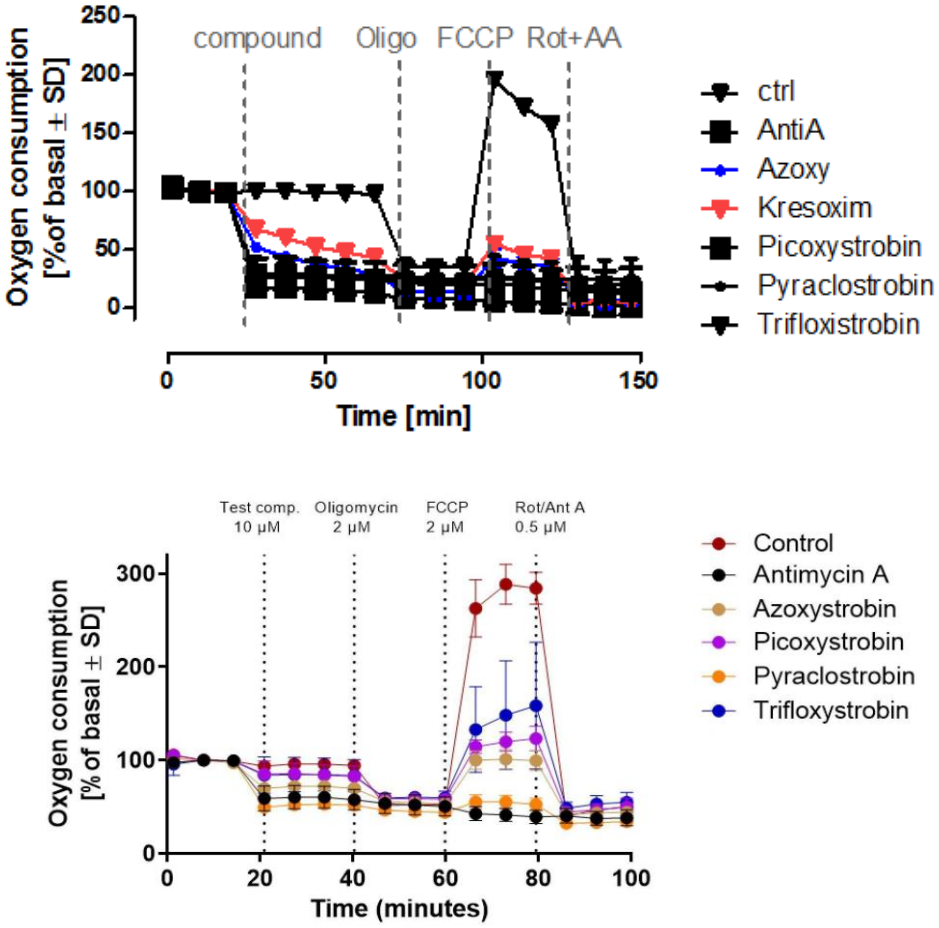


Mitochondrial dysfunction of intact cells was assessed through quantification of oxygen consumption of intact LUHMES and RPTEC/TERT1 cells.
LHUMES: An acute injection of a high, non-cytotoxic concentration (antimycin A, azoxystrobin, picoxystrobin: 50 µM; kresoxim-methyl: 12.5 µM; pyraclostrobin and trifloxystrobin: 20 µM) completely inhibited cellular mitochondrial oxygen consumption. Except from azoxystrobin and kresoxim-methyl, where a minor respiration was still detectable after 50 min treatment, all tested CIII inhibitors inhibited mitochondrial oxygen consumption directly and maximally.

RPTEC/TERT1: Differentiated RPTEC/TERT1 cells were injected with 10 µM of test compound, oxygen consumption rates were measured for 20 minutes before and after injection. All compounds show to inhibit the oxygen consumption but to different extents. Antimycin A and pyraclostrobin gave a complete inhibition, followed by azoxystrobin, picoxystrobin and trifloxystrobin.
Additionally, oxygen consumption of HepG2 cells (a human hepatocarcinoma cell line) was assessed as well. The basal respiration of whole cells was measured for 20 minutes prior to injection of the test compound, and again after injection for 30 minutes exposure. Changes in OCR upon compound administration give a direct and specific observation of effects of test substance in basal mitochondrial function.
In conclusion, the target compound, azoxystrobin, caused less potent effects on mitochondrial oxygen consumption than the source compounds picoxy- and pyraclostrobin, in the two models as already seen in the individual complex activity assay in LUHMES. This might be due to the predicted lower intracellular concentration of azoxystrobin (see below) compared to the source compounds.

**Figure 5.5. Mitochondrial dysfunction was assessed measuring the oxygen consumption rates of intact HepG2 cells.**

Oxygen consumption rates were measured prior to compound injection for 20 min, and after acute injection of toxins for 30 min. Data are quantified relative to basal oxygen consumption rates. Results are mean ± SD of one experiment with 2 technical replicates.

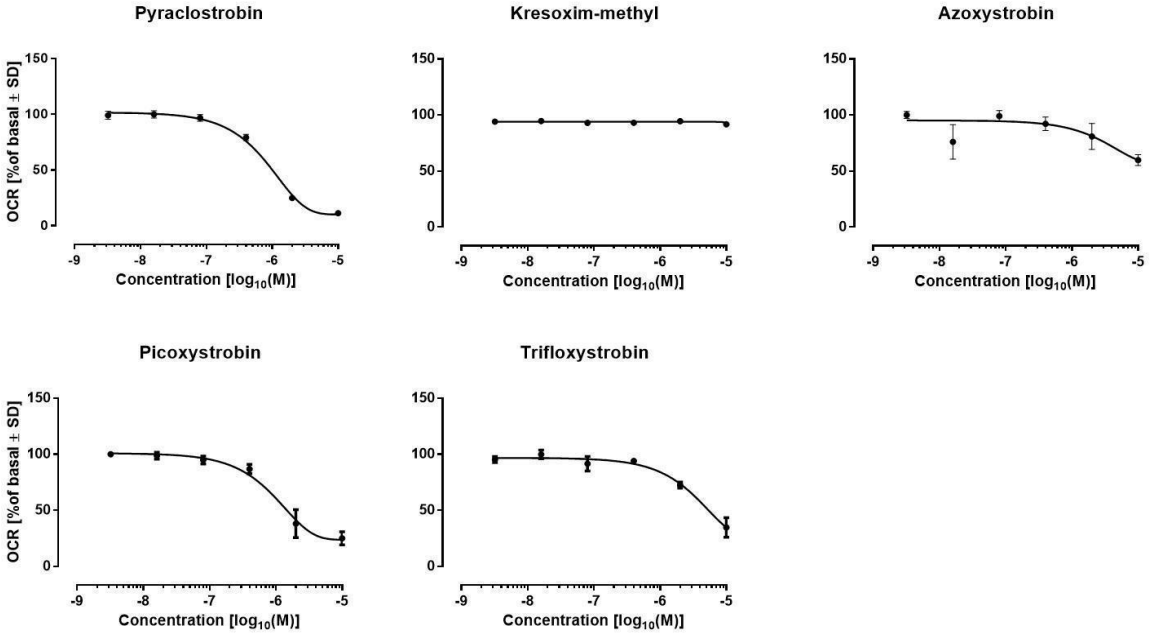


## 2. *Effects on mitochondrial membrane potential (MMP)*

To assess the effects on mitochondrial integrity upon chemical exposure, the presences of the membrane potential in mitochondria was measured using the potential dependent dyes Rhodamine123 or JC-1. Rhodamine123 will diffuse into mitochondria with a potential. A decrease or absence of potential leads to a decrease or absence of dye. In the case of the JC-1 dye, the presence of a potential leads to accumulation of the dye into the mitochondria.

High concentration of the dye form aggregates and emits light with a wavelength around 561 nm while the non-aggregated dye emits light around 488 nm.

The results indicate that the exposure to the reference compound Antimycin A has the most potent effect on MMP, when comparing to the effects upon exposure to the target compound azoxystrobin and all source compounds. Azoxystrobin exposure leads to a concentration-dependent decrease of the MMP comparable to picoxystrobin and pyraclostrobin for 2, 3 cell lines respectively. Both trifloxystrobin and kresoxim-methyl are less potent in inhibiting the MMP in at least two out of 3 cell lines. Only the neuronal cell line (SH-SY5Y) demonstrates a 50% decrease compared to control at the higher concentration. Antimycin A had as expected the highest potency.

**Figure 5.6. Assessment of mitochondrial dysfunction through quantification of mitochondrial membrane integrity in HepG2, RPTEC and SH-Sy5Y cells.**

The membrane integrity was quantified 24 h after compound (A; Antimycin A, B; Azoxystrobin, C; Kresoxim-methyl, D; Picoxystrobin, E; Pyraclostrobin, F; Trifloxystrobin) exposure based on Rho123 intensity in HepG2 and SH-SY5Y cells and based on JC-1 in RPTEC cells. Curves are an average biological replicates plus standard deviations. Missing graphs for cell lines means that there was no effect at the MMP.

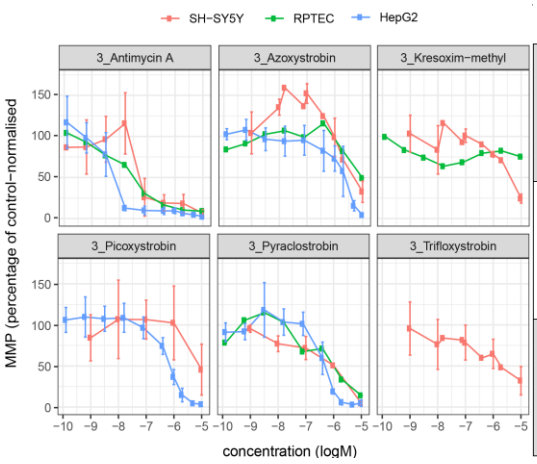


| | | HepG2 | RPTEC | SH-SY5Y |
|---|---|---|---|---|
| | | Log10 (M) | | |
| Antimycin A | BMR5 | -8,88 | -9,58 | -7,25 |
| | BMR10 | -8,71 | -9,05 | -7,22 |
| | BMR15 | -8,61 | -8,73 | -7,21 |
| | BMR20 | -8,53 | -8,48 | -7,19 |
| | BMR25 | -8,46 | -8,28 | -7,18 |
| | BMR30 | -8,4 | -8,1 | -7,17 |
| | BMR50 | -8,21 | -7,51 | -7,14 |
| Azoxystrobin | BMR5 | -6,57 | -5,77 | -5,98 |
| | BMR10 | -6,35 | -5,73 | -5,78 |
| | BMR15 | -6,22 | -5,71 | -5,66 |
| | BMR20 | -6,11 | -5,69 | -5,57 |
| | BMR25 | -6,03 | -5,67 | -5,49 |
| | BMR30 | -5,95 | -5,66 | -5,42 |
| | BMR50 | -5,7 | -5,49 | -5,2 |
| Kresoxim-methyl | BMR5 | NA | NA | -6.62 |
| | BMR10 | NA | NA | -6.32 |
| | BMR15 | NA | NA | -6.14 |
| | BMR20 | NA | NA | -6 |
| | BMR25 | NA | NA | -5.88 |
| | BMR30 | NA | NA | -5.78 |
| | BMR50 | NA | NA | -5.44 |

| | | HepG2 | RPTEC | SH-SY5Y |
|---|---|---|---|---|
| | | Log10 (M) | | |
| Picoxystrobin | BMR5 | -6,88 | NA | -5,86 |
| | BMR10 | -6,69 | NA | -5,83 |
| | BMR15 | -6,58 | NA | -5,81 |
| | BMR20 | -6,49 | NA | -5,8 |
| | BMR25 | -6,41 | NA | -5,79 |
| | BMR30 | -6,35 | NA | -5,78 |
| | BMR50 | -6,14 | NA | -5,74 |
| Pyraclostrobin | BMR5 | -6,93 | -7,86 | -8,81 |
| | BMR10 | -6,77 | -7,41 | -8,19 |
| | BMR15 | -6,68 | -7,12 | -7,81 |
| | BMR20 | -6,6 | -6,91 | -7,52 |
| | BMR25 | -6,54 | -6,74 | -7,28 |
| | BMR30 | -6,49 | -6,59 | -7,07 |
| | BMR50 | -6,31 | -6,07 | -6,37 |
| Trifloxystrobin | BMR5 | NA | NA | -8,2 |
| | BMR10 | NA | NA | -7,67 |
| | BMR15 | NA | NA | -7,27 |
| | BMR20 | NA | NA | -6,94 |
| | BMR25 | NA | NA | -6,65 |
| | BMR30 | NA | NA | -5,68 |
| | BMR50 | NA | NA | NA |

## *3. Effects on glycolysis*

To assess the effect on overall function of the mitochondria, the capacity of the cell to undergo glycolytic switch was addressed based on the production of lactate. Inhibition of the various electron transport chain complexes will perturb the oxidative phosphorylation and force the cell to use glycolysis to deal with their energetic demand. The use of the glycolytic pathway leads to the increase of one of the endpoint metabolites, lactate. An increase of lactate concentration measured in the supernatant medium indicates an increase in glycolytic rates.

The results indicate that exposure to the target compound azoxystrobin leads to an increase in lactate production in a similar manner as the source compounds pyraclostrobin, picoxystrobin and the reference compound antimycin A in both renal and hepatic models. The same but to a lower extent can be seen for the neuronal cell model SH-SY5Y. The degree of complex III inhibition induced glycolytic switch of azoxystrobin is shown to be lower than the before mentioned source compounds but higher then kresoxim-methyl and trifloxystrobin, which resulted in low or no stress induction. This might be due to the predicted lower intracellular concentration of azoxystrobin (see below) compared to the source compounds.

**Figure 5.7. Assessment of mitochondrial function downregulation by measurement of lactate as indicator of glycolytic switch.**

Left) Supernatant lactate was measured in RPTEC/TERT1 and HepG2 cells after 24 h exposure to a range of concentrations of different strobilurins. Data are represented as percentage of 0.1%DMSO controls and re-normalised to the average of at least two no-effect concentrations (if applicable).

Right) ECs relative to increased lactate production reduction calculated in re-normalised data sets using the point-to-point extrapolation method

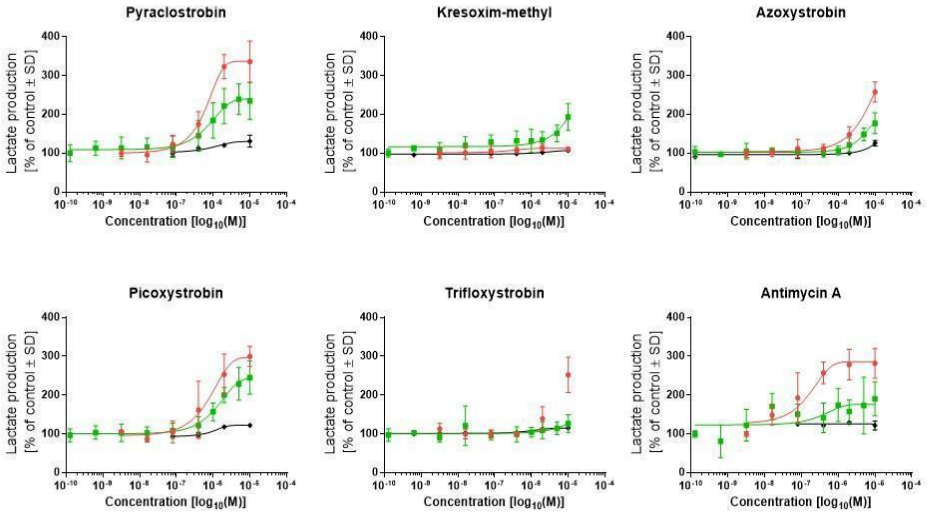


RPTEC/TERT1
HepG2
SH-SY5Y

| | | RPTEC/TERT1 | HepG1 | SH-SY5Y | | | RPTEC/TERT1 | HepG1 | SH-SY5Y |
|---|---|---|---|---|---|---|---|---|---|
| | | $log_{10}$(M) | | | | | $log_{10}$(M) | | |
| Pyraclostrobin | EC5 | -6.79079 | -7.48503 | -6.57052 | Picoxystrobin | EC5 | NA | -7.07653 | -5.9903 |
| | EC10 | -6.73801 | -7.18485 | -6.41893 | | EC10 | -6.70983 | -6.87339 | -5.8479 |
| | EC15 | -6.69096 | -7.00904 | -6.09609 | | EC15 | -6.5797 | -6.61474 | -5.7409 |
| | EC20 | -6.64852 | -6.88425 | -5.70283 | | EC20 | -6.51955 | -6.4475 | -5.2387 |
| | EC25 | -6.60985 | -6.74758 | -5.26062 | | EC25 | -6.48084 | -6.33931 | NA |
| | EC30 | -6.57435 | -6.62992 | -5.03773 | | EC30 | -6.44529 | -6.26497 | NA |
| | EC50 | -6.41676 | -6.32084 | NA | | EC50 | -6.32029 | -6.05296 | NA |
| Kresoxim-methyl | EC5 | -6.57595 | -7.6182 | -5.16249 | Trifloxystrobin | EC5 | -6.6522 | -5.96528 | -6.1461 |
| | EC10 | -5.96817 | -7.31832 | NA | | EC10 | -6.76767 | -5.63569 | -5.8123 |
| | EC15 | NA | -7.14262 | NA | | EC15 | -5.9311 | -5.28468 | -5.003 |
| | EC20 | NA | -7.01787 | NA | | EC20 | -5.86276 | -5.14221 | NA |
| | EC25 | NA | -6.92108 | NA | | EC25 | -5.80373 | -5.03511 | NA |
| | EC30 | NA | -6.68728 | NA | | EC30 | -5.75177 | NA | NA |
| | EC50 | NA | -5.31629 | NA | | EC50 | -5.53702 | NA | NA |
| Azoxystrobin | EC5 | -7.3559 | -8.13409 | -5.47104 | Antimycin A | EC5 | -6.83082 | -7.83798 | NA |
| | EC10 | -7.12703 | -5.91329 | -5.30381 | | EC10 | -6.81165 | -7.53887 | NA |
| | EC15 | -6.28919 | -5.80256 | -5.18338 | | EC15 | -6.79329 | -7.36342 | NA |
| | EC20 | -6.12977 | -5.7144 | -5.08919 | | EC20 | -6.77568 | -7.2388 | NA |
| | EC25 | -6.01341 | -5.61342 | -5.01184 | | EC25 | -6.75876 | -7.14208 | -6.7084 |
| | EC30 | -5.92173 | -5.52613 | NA | | EC30 | -6.74246 | -7.06303 | NA |
| | EC50 | -5.66361 | -5.281 | NA | | EC50 | -6.6828 | -6.25049 | NA |

### *KE3: neuronal degeneration*

#### *1. Effects on cell viability*

To assess chemical induced cellular damage, cell viability was measured by determining metabolic reduction activity using the redox indicator resazurin in RPTEC/TERT1, HepG2, LUHMES and SH-SY5Y cells, for 1.5 h after 24 h exposure of compounds.

The results show that at tested concentrations of strobilurins no cytotoxicity was observed in the hepatic (HepG2) and neuronal (LUHMES, SH-SY5Y) models after 24 h of exposure. However, the highest concentration of antimycin A showed a decrease of about 80% in viability (i.e. cytotoxicity) in LUHMES cells at 50 µM and 20% in SH-SY5Y at 10 µM. With the same conditions, viability of kidney cells RPTEC/TERT1 is shown to be affected in a manner that is proportional inverted to the lactate production in the same cell line, indicating that the loss of viability is directly correlated with impaired oxidative phosphorylation due to complex III inhibition.

The effect of target compound azoxystrobin is comparable to the ones of source compounds in all four cell types, corroborating the degree of the read across prediction.

**Figure 5.8. Effect of selected strobins on viability assessed with resazurin assay.**

Left) RPTEC/TERT1, HepG2, LUHMES and SH-SY5Y cells were exposed to chemicals for 24 h. Resazurin reduction capacity was measured after exposure and quantified relative to 0.1% DMSO control samples. All data were re-normalised to the average of at least two no-effect concentrations (if applicable).

Right) BMRs of selected strobins relative to resazurin reduction calculated in re-normalised data sets using the *in vitro* toxicology on-line tool provided by AG. Leist, University of Konstanz.

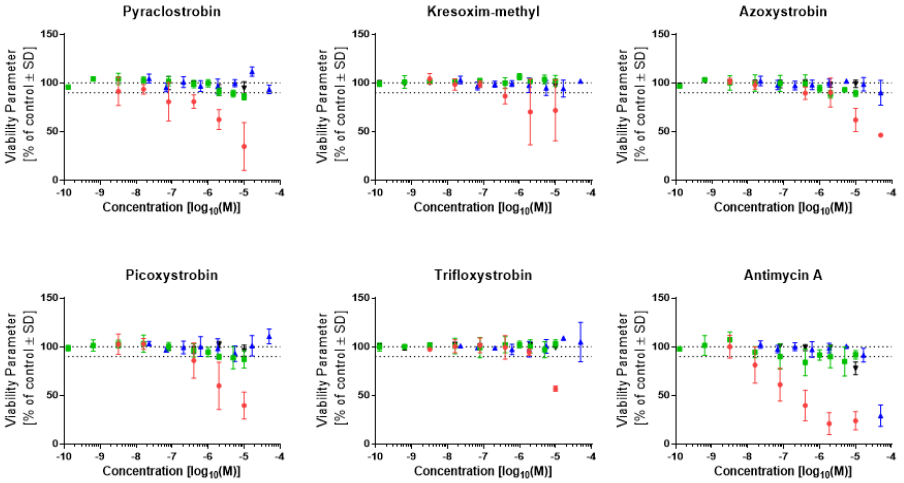


RPTEC/TERT1
HepG2
LUHMES
SH-SY5Y

| | | RPTEC/TERT1 | HepG2 | LUHMES | SH-SY5Y |
|---|---|---|---|---|---|
| | | log10(M) | | | |
| Pyraclostrobin | BMR5 | -7.83 | -5.81 | NA | -5.35 |
| | BMR10 | -7.24 | -5.66 | NA | NA |
| | BMR15 | -6.87 | NA | NA | NA |
| | BMR20 | -6.59 | NA | NA | NA |
| | BMR25 | -6.36 | NA | NA | NA |
| | BMR30 | -6.16 | NA | NA | NA |
| | BMR50 | -5.49 | NA | NA | NA |
| Kresoxim-methyl | BMR5 | -6.61 | NA | NA | NA |
| | BMR10 | -6.47 | NA | NA | NA |
| | BMR15 | -6.37 | NA | NA | NA |
| | BMR20 | -6.26 | NA | NA | NA |
| | BMR25 | -6.11 | NA | NA | NA |
| | BMR30 | NA | NA | NA | NA |
| | BMR50 | NA | NA | NA | NA |
| Azoxystrobin | BMR5 | -6.61 | -6.04 | NA | NA |
| | BMR10 | -6.08 | NA | NA | NA |
| | BMR15 | -5.75 | NA | NA | NA |
| | BMR20 | -5.51 | NA | NA | NA |
| | BMR25 | -5.3 | NA | NA | NA |
| | BMR30 | -5.12 | NA | NA | NA |
| | BMR50 | NA | NA | NA | NA |

| | | RPTEC/TERT1 | HepG2 | LUHMES | SH-SY5Y |
|---|---|---|---|---|---|
| | | log10(M) | | | |
| Picoxystrobin | BMR5 | -6.77 | -6.13 | NA | NA |
| | BMR10 | -6.5 | -5.64 | NA | NA |
| | BMR15 | -6.32 | NA | NA | NA |
| | BMR20 | -6.18 | NA | NA | NA |
| | BMR25 | -6.06 | NA | NA | NA |
| | BMR30 | -5.95 | NA | NA | NA |
| | BMR50 | -5.47 | NA | NA | NA |
| Trifloxystrobin | BMR5 | -5.73 | NA | NA | NA |
| | BMR10 | -5.52 | NA | NA | NA |
| | BMR15 | -5.4 | NA | NA | NA |
| | BMR20 | -5.3 | NA | NA | NA |
| | BMR25 | -5.22 | NA | NA | NA |
| | BMR30 | -5.15 | NA | NA | NA |
| | BMR50 | NA | NA | NA | NA |
| Antimycin A | BMR5 | -8.13 | -7.81 | -4.86 | -5.31 |
| | BMR10 | -7.86 | -7.61 | -4.75 | -5.18 |
| | BMR15 | -7.69 | NA | -4.68 | -5.09 |
| | BMR20 | -7.56 | NA | -4.63 | -5.02 |
| | BMR25 | -7.44 | NA | -4.59 | NA |
| | BMR30 | -7.34 | NA | -4.55 | NA |
| | BMR50 | -6.92 | NA | -4.43 | NA |

### *Effect on neurite outgrowth (LUHMES)*

The degeneration of dopaminergic nigrastriatal cells was assessed by the NeuriTox test. This is a test that was established to identify neurotoxic compounds (Stiegler *et al.*, 2011; Krug *et al.*, 2013; Delp 2018). Cells are treated for 24 h during their differentiation (d2-3) and neurite outgrowth is assessed subsequently. Substances that specifically impair neurite outgrowth at concentrations >=4 times lower than they cause general cytotoxicity, are classified as specific neurotoxicants.

**Figure 5.9. Assessment of neurite outgrowth inhibition of differentiating LUHMES dopaminergic neurons as established and predictive model for neurotoxicity.**

LUHMES cells differentiated for two days were plated at a density of 100,000 cells/cm² (ca. 30,000 cells/well) into 96-well plates, treated one hour later and analysed after 24 h. Neurite area (NA, orange) and viability (V, black) were determined by high content imaging. Resazurin reduction and intracellular ATP content were determined in parallel to neurite area and viability.

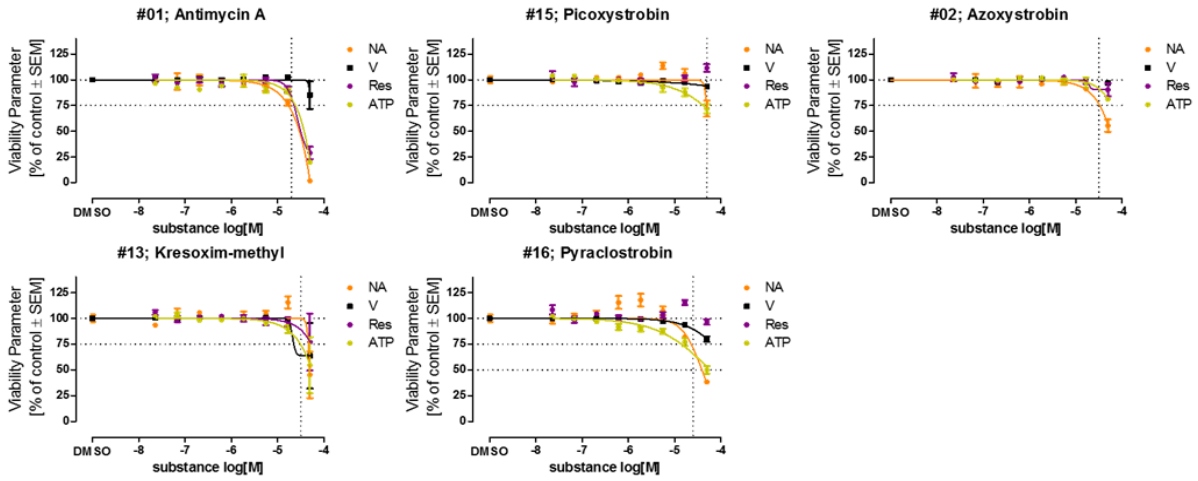


All tested strobilurins did not cause a specific inhibition of neurite outgrowth, nor did they affect viability strongly at concentrations up to 50 µM. Thus, it can be concluded that both, source and target compounds, inherit a comparable and low neurotoxicity hazard measured by the assay.

### *Repeat dosing scenarios*

### *1. Repeated dose toxicity (LUHMES)*

As *in vivo*, humans might not only be exposed to the toxicant once, but repeatedly, this scenario was modelled *in vitro*, accordingly. Technically, this was done by initiation of treatment on d5 of differentiation of the LUHMES cells, followed by a half-medium exchange on d7 and assay on d10. Thus, substances that were not stable *in vitro* or have certain physico-chemical properties that make them adhere stronger to membranes or plastic will be applied at higher doses, while for stable and hydrophilic substances, no difference should be introduced by the medium change and repeated dosing.

**Figure 5.10. Assessment of neurite integrity of LUHMES dopaminergic neurons.**

Cells differentiated for two days were plated at a density of 150,000 cells/cm² (ca. 45,000 cells/well) into 96-well plates, treated on day 5 and day 7 and analysed at day 10. Neurite area (NA, orange) and viability (V, black) were determined by high content imaging.

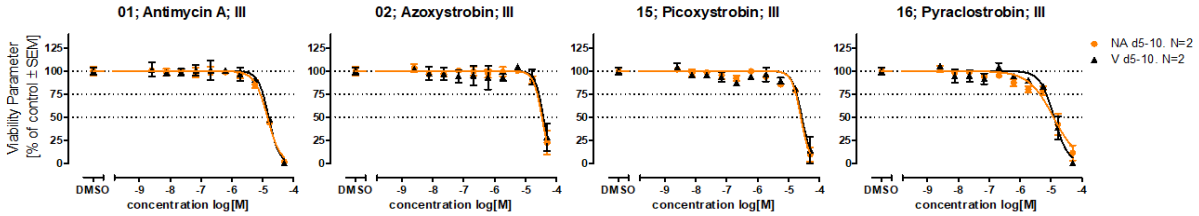


For concentrations up to 10 µM, no effect, neither on neurite integrity nor on viability, could be detected. For concentrations greater 10 µM, no differences between the strobilurins were present, thus the same hazard statement should apply to all of them. However, in this experimental setup the strobilurins behaved similar to antimycin A. An explanation could be that longer-term exposure to CIII inhibitors cause non-specific cell-damage.

## *2. Repeated dose toxicity (SH-SY5Y)*

The ATP content in SH-SY5Y cells was analysed after repeated (72h+48h) exposure. The endpoint reflects the respiratory capacity and number of viable cells per well. The results show that the decrease in ATP content follows the attenuated MMP (Figure 5.11).

**Figure 5.11. ATP content measured by the ATP luminescence CellTiter Glo assay in SH-SY5Y cells after exposure with compounds for 120h (72h+48h).**

The endpoint reflects the number of viable cells and mitochondrial activity. The cells were plated at a cell density of 8,000 cells/well and differentiated for 3 days prior exposure.

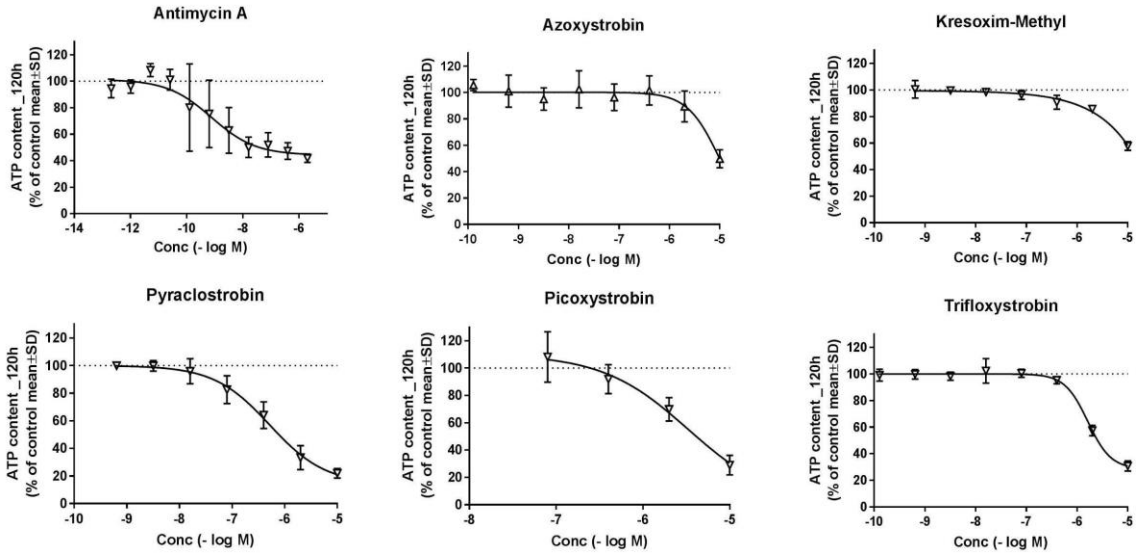

### *3. Neurite degeneration (SH-SY5Y). "Acute" and repeated dose exposure.*

To assess degeneration of dopaminergic neurons, the change in neurite length after exposure was evaluated in differentiated SH-SY5Y cells. The cells were differentiated for 6 or 3 days and treated with the selected chemicals for 24 or 120 hours, respectively. Successively, Calcein AM was used for staining the cytoplasm permitting the measurement of neurite length. Simultaneously, cytotoxicity was measured by propidium iodide exclusion after 24 or 120 hours of exposure. The results are expressed as the percentage of viable cells/mean neurite length in comparison to the DMSO controls.

**Figure 5.12. Neurite degeneration measured as mean neurite length and viability measured as propidium iodide exclusion in human neuroblastoma SH-SY5Y cells after exposure to compounds for 24 hrs or 120 h.**

The cells were plated at a cell density of 8,000 cells/well and differentiated for 6 or 3 days prior exposure for 24 hrs or 120 h, respectively.

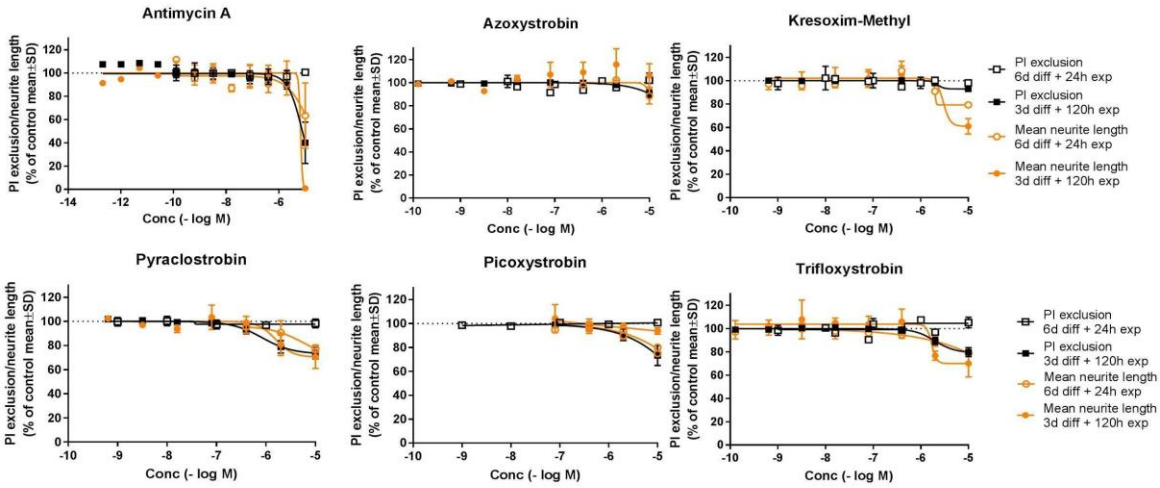


Azoxystrobin was negative in the neurite degeneration in SH-SYH5 cells (regardless of exposure scheme) while the other strobilurins showed weak activity.

### *4. Repeated dose toxicity (RPTEC/TERT1)*

To mimic the *in vivo* situation of a repeated exposure to a chemical, strobins (azoxystrobin, picoxystrobin and pyraclostrobin) and antimycin A, were applied to RPTEC/TERT1 cells in a repeated dose regime experiment. To test whether concentration of compounds that did not have an effect on the system in acute dose have an effect in repeated dose, cells were treated every 24 h with 4 concentrations of compounds, namely $EC_{20}$, NOEL, 1/3 NOEL and 1/9 NOEL according to the lactate production assay in acute dose regime (24h). Supernatant lactate was measured every day and viability was assessed at day 5 with resazurin reduction assay.

**Figure 5.13. Top) Lactate production changes overtime after repeated dose of compound. Middle) Viability assessed on day 5 with resazurin assay for the four concentrations. Bottom) Respective concentrations of $EC_{20}$, NOEL, ⅓ NOEL and 1/9 NOEL for relative compounds.**

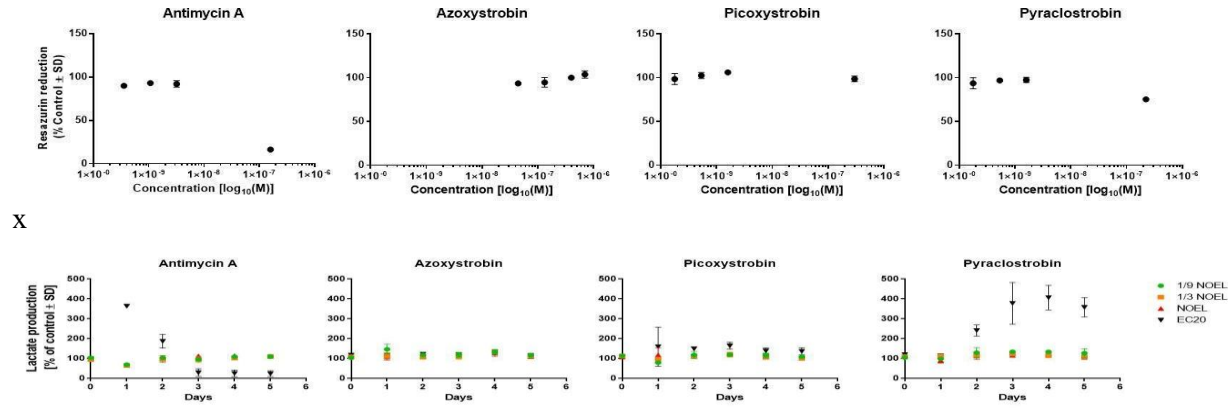


| | | 1/9 NOEL | 1/3 NOEL | NOEL | EC20 |
|---|---|---|---|---|---|
| Antimycin A | [M] | 3.56E-10 | 1.07E-09 | 3.20E-09 | 1.60E-07 |
| Azoxystrobin | [M] | 4.44E-08 | 1.33E-07 | 4.00E-07 | 7.00E-07 |
| Picoxystrobin | [M] | 1.78E-10 | 5.33E-10 | 1.60E-09 | 3.00E-07 |
| Pyraclostrobin | [M] | 1.78E-10 | 5.33E-10 | 1.60E-09 | 2.24E-07 |

For none of the non-effective concentrations of compounds in acute dose regime there was an effect in repeated dose regime. Repeated dose of antimycin A decreased the lactate production starting from day 2, probably due to cell death assessed on day 5. No further increase in lactate production or decrease in viability were found in repeated exposure of azoxystrobin and picoxystrobin compared to acute exposure, whereas increased lactate production by pyraclostrobin exposure reached a peak on day 4 and decreased again on day 5 due to loss in viability as shown in resazurin reduction on day 5.

### *In vitro in silico model (cellular bioavailability)*

*In silico* biokinetics were predicted using the methods developed in the EU-Tox risk project (see annex for method details). The predictions for each compound in the various test systems are shown below.

**Table 5.5. Predictions for HEPG2-HULAFE after a nominal application of 1 µM.**

| Compound | Predicted Concentration (M) | | Nominal:cell concentration ratio |
|---|---|---|---|
| | Media | Cell | |
| Antimycin-A | 2.78E-08 | 1.54E-05 | 15.4 |
| Azoxystrobin | 8.75E-07 | 6.21E-06 | 6.2 |
| Kresoxim methyl | 4.33E-07 | 2.32E-05 | 23.2 |
| Picoxystrobin | 3.18E-07 | 2.72E-05 | 27.2 |
| Pyraclostrobin | 1.51E-07 | 3.21E-05 | 32.1 |
| Trifloxystrobin | 4.81E-08 | 3.35E-05 | 33.5 |

**Table 5.6. 6Predictions for HEPG2-LEIDEN after a nominal application of 1 µM**

| Compound | Predicted Concentration (M) | | Nominal:cell concentration ratio |
|---|---|---|---|
| | Media | Cell | |
| Antimycin-A | 2.43E-08 | 1.35E-05 | 13.5 |
| Azoxystrobin | 8.40E-07 | 5.96E-06 | 6.0 |
| Kresoxim methyl | 3.75E-07 | 2.01E-05 | 20.1 |
| Picoxystrobin | 2.70E-07 | 2.30E-05 | 23.0 |
| Pyraclostrobin | 1.25E-07 | 2.65E-05 | 26.5 |
| Trifloxystrobin | 3.97E-08 | 2.77E-05 | 27.7 |

**Table 5.7. Predictions for LUHMES after a nominal application of 1 µM**

| Compound | Predicted Concentration (M) | | Cell:nominal concentration ratio |
|---|---|---|---|
| | Media | Cell | |
| Antimycin-A | 3.09E-07 | 3.61E-04 | 361.0 |
| Azoxystrobin | 9.85E-07 | 1.45E-05 | 14.5 |
| Kresoxim methyl | 8.96E-07 | 1.03E-04 | 103.0 |
| Picoxystrobin | 8.48E-07 | 1.54E-04 | 154.0 |
| Pyraclostrobin | 7.00E-07 | 3.15E-04 | 315.0 |
| Trifloxystrobin | 4.14E-07 | 6.11E-04 | 611.0 |

**Table 5.8. Predictions for RPTEC after a nominal application of 1 µM**

| Compound | Predicted Concentration (M) | | Nominal:cell concentration ratio |
|---|---|---|---|
| | Media | Cell | |
| Antimycin-A | 1.40E-07 | 4.94E-05 | 49.4 |
| Azoxystrobin | 9.37E-07 | 4.36E-06 | 4.4 |
| Kresoxim methyl | 6.69E-07 | 2.29E-05 | 22.9 |
| Picoxystrobin | 5.62E-07 | 3.06E-05 | 30.6 |
| Pyraclostrobin | 3.43E-07 | 4.62E-05 | 46.2 |
| Trifloxystrobin | 1.37E-07 | 6.06E-05 | 60.6 |

**Table 5.9. Predictions for SHSY5Y after a nominal application of 1 µM**

| Compound | Predicted Concentration (M) | | Nominal:cell concentration ratio |
|---|---|---|---|
| | Media | Cell | |
| Antimycin-A | 1.55E-07 | 1.81E-04 | 181.0 |
| Azoxystrobin | 9.47E-07 | 1.40E-05 | 14.0 |
| Kresoxim methyl | 6.99E-07 | 8.00E-05 | 80.0 |
| Picoxystrobin | 5.96E-07 | 1.08E-04 | 108.0 |
| Pyraclostrobin | 3.75E-07 | 1.69E-04 | 169.0 |
| Trifloxystrobin | 1.54E-07 | 2.28E-04 | 228.0 |

**Table 5.10. Predictions for U20S after a nominal application of 1 µM**

| Compound | Predicted Concentration (M) | | Nominal:cell concentration ratio |
|---|---|---|---|
| | Media | Cell | |
| Antimycin-A | 4.46E-08 | 1.00E-05 | 10.0 |
| Azoxystrobin | 9.12E-07 | 1.85E-06 | 1.9 |
| Kresoxim methyl | 5.42E-07 | 9.11E-06 | 9.1 |
| Picoxystrobin | 4.23E-07 | 1.17E-05 | 11.7 |
| Pyraclostrobin | 2.22E-07 | 1.64E-05 | 16.4 |
| Trifloxystrobin | 7.65E-08 | 2.06E-05 | 20.6 |

In all models, the intracellular concentration are modelled to be approx. similar amongst the strobilurins within one order of magnitude. Nevertheless, for all predictions, azoxystrobin shows somewhat lower intracellular concentrations. Azoxystrobin's relatively low log P results in the lower concentrations predicted. This supports the assumption that the compounds are equipotent, in that higher treatment concentrations (doses) would be required to observe comparable toxicity, see below.

PBPK simulations were conducted in both rat and human for all of the compounds. The results are summarised below and described in detail in the annex.

**Table 5.11. *In silico* ADME prediction in humans**

| Compounds | Permeability | Absorption | Distribution | Metabolism | Clearance |
|---|---|---|---|---|---|
| Azoxystrobin | High | High | Moderate | Extensive | Moderate |
| Pyraclostrobin | High | Moderate | Moderate | Extensive | Low |
| Picoxystrobin | High | High | Moderate | Extensive | Low |
| Trifloxystrobin | High | Low | Moderate | Extensive | Moderate |
| Kresoxim-methyl | High | Moderate | Moderate | Extensive | High |
| Antimycin A | High | Low | Moderate | Extensive | Low |

## *PBPK*

### *1. Predictions in humans*

The compounds have a range of lipophilicity values and azoxystrobin is the least lipophilic of the compounds, thus indicating the lowest potential to cross the blood-brain barrier. The measured human protein binding showed a trend for fraction unbound (fu) to increase with Log P with azoxystrobin having the lowest protein binding (highest fu). In the absence of solubility limitations all of the compounds were predicted to have reasonable passive membrane permeability and to have almost complete absorption (fa for all compounds >0.9). There was a relationship between Log P and solubility for the strobilurin compounds with azoxystrobin having the highest solubility. Using default values for precipitation rate constant and supersaturation ratios, the human absorption of the strobilurins compounds was predicted. At a dose of 10 mg/kg orally only azoxystrobin and picoxystrobin were predicted to have high absorption. Although there is some uncertainty about the correct values to use for these parameters the overall conclusion from these analyses is that azoxystrobin and picoxystrobin are likely to have higher oral absorption at high doses in humans than the other case study compounds.

The predicted distribution of all of the compounds was consistent across the different prediction methods tested. All of the compounds had moderate predictions of volume of distribution that were higher than total body water (0.6 L/kg) indicating that the compounds

distribute into the tissues. The distribution was also predicted to be similar in the rat. It is assumed that a potential neurotoxic effect would arise from exposure to local concentrations in the brain. The predicted steady-state brain to plasma distribution ratio was predicted to be 0.4 to 3.9 in the rat across the series of compounds and between 0.98 and 4.4 in humans. Azoxystrobin was in the middle of the range in both species with the brain concentration being predicted to be about 2-fold of those in plasma in both rat and human.

*In vitro-in vivo* extrapolation of the human metabolic clearance of this series of compounds resulted in a wide range of predicted clearance values (table 13 of annex). Azoxystrobin has the shortest predicted half-life of all of the compounds and was simulated to be significantly removed from the body over 72 hours after an intravenous dose of 10mg/kg and therefore it may be expected to have less effects. When the unbound concentrations were considered, azoxystrobin has the highest initial plasma concentrations but due to the short predicted half-life the concentrations are the lowest by the end of the simulation period.

## *2. Simulated rat pharmacokinetics*

The clearance of the strobilurin case study chemicals was predicted in the rat using an allometric approach to scale down the human clearance. This leads to a wide range of predicted clearance values in the rat. These values were used as input in the physiologically based pharmacokinetic (PBPK) model in the rat and simulations of oral doses were made and compared to any available pharmacokinetic data in the rat.

For pyraclostrobin, the fraction and rate of absorption were consistent with data obtained dosing 5 or 50 mg/kg to the animals. Consistent with the radiolabel data the majority of the compound is eliminated within 48 hours, however, the predicted plasma exposure in the rat is higher than the observed radiolabel AUC. This suggests that the clearance of pyraclostrobin in the rat is underpredicted using the technique of back extrapolation from human and may suggest that the rate of metabolism is much faster in rats than humans or that the protein binding of pyraclostrobin in the rat is lower than the predicted value used in the simulation. Unfortunately, it is not possible to generate metabolism data in rat hepatocytes or protein binding in rat plasma under the auspices of the EU-ToxRisk project to distinguish these hypotheses. Regardless, the discrepancy between simulated and observed data described herein suggests that the simulated pyraclostrobin data should be used with caution in the read across exercise.

For trifloxystrobin, kresoxim methyl, azoxystrobin and picoxystrobin the rat PBPK models were consistent with available pharmacokinetic data. For antimycin A, no observed pharmacokinetic data in the rat was found in the literature. The pharmacokinetics of all of the case study chemicals were predicted at oral doses of 10 and 100 mg/kg .The total concentrations of azoxystrobin were within the range of simulated concentrations of the other compounds. However, when the free plasma concentrations were considered, azoxystrobin has the highest unbound maximum concentration in plasma ($C_{max}$) but due to the rapid clearance and short half-life the steady state concentrations were lower than but similar to those of picoxystrobin.

With the stated assumptions around linearity of clearance and fraction unbound the concentrations of azoxystrobin and picoxystrobin were compared across a range of doses up to 2000 mg/kg. The average steady state total plasma concentration of azoxystrobin were lower and the unbound steady state plasma concentrations were comparable to those

of picoxystrobin. The $C_{max}$ (total and unbound) concentrations of azoxystrobin were higher than those of picoxystrobin.

## 5.2. Justification

The existing *in vivo* ADME data indicated that the target as well as the source compounds has limited distribution to the brain (whole brain). The predicted steady-state brain to plasma distribution ratio was predicted to be 0.4 to 3.9 in the rat across the series of compounds and between 0.98 and 4.4 in humans. Azoxystrobin was in the middle of the range in both species with the brain concentration being predicted to be about 2-fold of those in plasma in both rat and human.

The data obtained on the inhibition of the individual complex activity was in line with the inhibition of total mitochondrial respiration of intact cells. Both methods showed that the target azoxystrobin resulted in comparable results as the source compounds. Furthermore, azoxystrobin appears to be less potent than the source compounds. These findings were also supported by NeuriTox test, which resulted in a "non neurotoxicant" classification for the source and target compounds.

Antimycin A and the strobilurins attenuated the mitochondrial membrane potential (MMP) in SH-SY5Y neuronal cells after 24h exposure with 10 µM. The decrease in MMP was followed by a decrease in the total ATP content per well, measured after 120h. A slight increase in extracellular lactate after 24h exposure indicates that there was a switch to glycolytic activity. Despite the attenuated mitochondrial activity, no cytotoxicity was observed after 24h exposure as measured by resazurin activity and propidium iodide (PI) exclusion. Only moderate cytotoxicity (<20% increase in PI stained cells) was observed after 120h exposure. Antimycin A and to a minor extent kresoxim-methyl, pyraclostrobin, picoxystrobin and trifloxystrobin reduced the mean neurite length at non-cytotoxic concentrations. Azoxystrobin was negative in the neurite degeneration assay. In conclusion, the target compound azoxystrobin was less active than the source compounds on the ATP content, neurite length and cell viability.

Antimycin A is most potent in attenuating the mitochondrial membrane potential (MMP) at 24h in all cell lines tested. Azoxystrobin demonstrated a similar concentration-response curve as picoxystrobin and pyraclostrobin. These findings indicate that based on the MMP predicts that azoxystrobin will induce similar effects upon cells as the other source compounds as expected.

The lactate production data indicates that the response obtained by exposure with the target compound azoxystrobin is similar to the one obtained with the source compounds and antimycin A. The extent of the induced stress resulted to be higher in azoxystrobin when compared to kresoxim-methyl and trifloxystrobin, and lower when compared to picoxystrobin and pyraclostrobin. Viability data according to the resazurin reduction capacity shows no cytotoxicity at tested concentrations for HepG2, LHUMES and SH-SY5Y for strobins, whereas RPTEC/TERT1 were the most affected. Furthermore, the sensitivity to the different compounds was maintained within the cell lines representing different tissues. In conclusion, the comparability of effects between the target and source compounds in terms of glycolytic switch and loss of viability is in line with the read across prediction hypothesis.

# 6. Strategy for and integrated conclusion of data gap filling

## 6.1. Uncertainty

**Table 6.1. Uncertainty assessment**

| Factor | Uncertainty | Comment |
|---|---|---|
| Structural boundary of the read across | Low for toxicodynamics, | The selected source and target chemical belong to the group of strobilurins. They have a common toxophore and binding site. The toxicity potential of the chemicals could depend on the type of substituents (In terms of structural similarity there is quite a difference). |
| | Medium for toxicokinetics | These substituents could affect the various ADME properties of the chemical. However, based on *in vivo* and simulation data the ADME properties are comparable. |
| Mode of action/AOP | Low for the MOA | The strobilurins are fungicides designed to inhibit the fungal complex III and with that reduce fungi multiplication. The toxicity potential in other species can be affected by the specificity of the chemical for mitochondrial complex III. However, it is known that the gene sequence for the various mitochondrial complexes are well preserved between species. The inhibition of complex III measured based on the mitochondrial respiration in isolated mitochondrial complexes demonstrated an efficient blocking of the complex III. |
| | Medium for the AOP, since the AOP is not yet defined/ validated | The proposed chain of events (possible AOP) has not yet been completely established and thoroughly reviewed. However, experimental evidence from *in vivo* and *in vitro* assays indicate the potential of the proposed AOP for the well-established complex III inhibitor antimycin A. However, the evidence regarding the Adverse Outcome in itself is sparse as little *in vivo*/human data is readily available. |
| Hypothesis | low | The uncertainty regarding the low neurotoxic potential of the source compounds is considered low, since no indication of neurotoxicity has been observed in numerous studies supported by toxicokinetic data showing little distribution to the brain.<br>The uncertainty regarding whether the complex III inhibition can induce neurotoxicity is medium to high since the strobilurins do not induce neurotoxicity. However, the mode of action has been established for antimycin A.<br>The chosen NAM methods support the hypothesis and they cover toxicodynamic and toxicokinetic endpoints and thus the uncertainty is considered low. |
| Structural similarity of source chemicals for read-across | low | For the Strobilurins it is likely that the selected analogues are suitable for read across, because of the common toxophore. The similarity of all selected analogues is high based on their common mode of action (mitochondrial complex III inhibition) |
| | Low | Despite of little chemichal similarity outside the toxophore, the similarity based on overall structure is considered high based on 3D-similaritites |
| Phys/Chem | Medium | The molecular weights and H-bond donor and acceptor properties are comparable between the target and the source compounds. However, the target compound has a relatively lower LogP value than the source compounds, thus the compound has less bio-accumulating capacity. Overall, this reduces the uncertainty regarding whether the target compound reaches the brain. |
| Toxicokinetics | *In vivo*: Low | Acceptable regulatory studies are available for the target and source compounds. The target compound as well as the source compounds have relatively high clearance with a vast metabolism. Also, the distribution to the brain is lower up to twice for azoxystrobin compared to the plasma concentration. |

<table>
<tr><td></td><td>In silico:</td><td>For some parameters within the azoxystrobin PBPK model there is uncertainty as to what is the correct input value to use. For these parameters, a sensitivity analysis was conducted and the impact on the simulation results (plasma exposure as judged by the area under the plasma concentration time profile) was evaluated.<br><br>
<table>
<tr><td colspan="2"></td><td>UNCERTAINTY</td><td></td><td></td></tr>
<tr><td colspan="2"></td><td>High</td><td>Medium</td><td>Low</td></tr>
<tr><td rowspan="3">SENSITIVITY</td><td>High</td><td>IV CL</td><td>Fu hepatic</td><td>In vitro Clint<br>Plasma fu<br>HPGL<br>Liver weight</td></tr>
<tr><td>Medium</td><td></td><td>Precipitation rate constant</td><td>Solubility</td></tr>
<tr><td>Low</td><td>Plasma fu</td><td>Super-saturation ratio</td><td>BP ratio</td></tr>
</table>
In vitro clint: intrinsic rate of metabolism<br>
Fu: fraction unbound<br>
IV CL: Clearance – intra-venous<br>
BP: Brain/plasma ratio<br>
HPGL: Hepatocellularity per gram of liver<br><br>
Parameter sensitivity and uncertainty table for the effect of changing different model parameters on simulated total plasma AUC of azoxystrobin in humans and rats. Other parameters tested that the model was not sensitive to included cardiac output, hepatic and renal blood flow. Sensitivity analysis results are presented as high (absolute value greater than or equal to 0.5), medium (absolute value greater than or equal to 0.2 but less than 0.5) or low (absolute value greater than or equal to 0.1 but less than 0.2); parameters with sensitivities less than 0.1 are not listed. A sensitivity ratio of 1 implies that a 1% change in input of a parameter value leads to a 1% change in dose metric prediction. Uncertainty is a subjective assessment of how reliable the input parameters are. A formal uncertainty analysis as suggested in the WHO PBPK guidance is difficult to perform with a bottom up PBPK model as the ratio of median to 95th percentile reflects a measure of variability rather than true uncertainty as could be obtained if the PBPK model parameters were fitted to an observed dataset. Note: the in vitro Clint value (intrinsic rate of metabolism) is considered low uncertainty based on the fact that it is measured in vitro.</td></tr>
<tr><td>Similarity of supportive data</td><td>low</td><td>in vivo<br>The used in vivo support is obtained using regulatory accepted data/methods. The selected analogues demonstrated comparable outcomes concerning the studied end point, but also similarities in the critical effects. there is some residual uncertainty since not all the source compounds had TG 424 neurotoxicity data.</td></tr>
<tr><td></td><td>medium -</td><td>In vitro</td></tr>
</table>

| | | |
|---|---|---|
| | | The literature indicates that different cell models and *Xenopus laevis* (adult and larvea) are adversely affected by azoxystrobin and other strobilurins at concentrations ≤1µM. *Xenopus laevis* larvae are more sensitive than adult fish. Genome expression in primary mouse cortical neuron cultures after exposure with the source compounds pyraclostrobin and trifloxystrobin indicates similarities that have been found in neurodegenerative and neurodevelopmental pathologies, but not in Parkinson's disease. The target compound azoxystrobin induced cytotoxicity at 1 µM but no correlation could be found in gene expression with correlation to neuronal disorders. |
| Number of analogues | Low/medium | The four selected analogues from the strobilurin show similar negative results. Only the selected AOP positive compound demonstrates a link to the proposed adverse outcome; neuronal toxicity. The number of negative analogues is enough to prove the similarity of the strobilurin. However, it is difficult to prove that the one selected AOP positive compound is enough to prove possible neuronal toxicity for other complex III inhibitors. |
| Quality of end point data | Low/medium | <u>Uncertainty of the assay</u><br>The different *in vitro* NAM methods used for addressing our read across case do not have an excepted guideline document. However, they all have a consortium wide reviewed description document. Finally, some of the assays are described in a DB-ALM document:<br>1. Seahorse, individual MRC complex activity = no DB-ALM (uncertainty = low).<br>2. Seahorse, mitochondrial respiration = no DB-ALM (uncertainty = low/medium).<br>3. ATP = created (not submitted) DB-ALM (uncertainty = low).<br>4. MMP = created DB-ALM (uncertainty = low)<br>5. Lactate assay = no DB-ALM (uncertainty = low)<br>6. Neurite outgrowth/NeuriTox = DB-ALM (uncertainty = low)<br>7. Neurite length = no DB-ALM (uncertainty = low)<br><br>All methods are internally validated. Various assay types are commonly used to address mitochondrial functioning in *in vitro* systems. The assays are performed in various laboratories. This can lead to differences in the execution concerning chemical usages, chemical exposures, data analysis, etc.<br>The different *In silico* NAM methods are not externally reviewed. Furthermore, we do not have enough *in vivo* data for this specific read across to completely validate the performance of the models. (uncertainty = high). |
| | High | <u>Following proposed AOP</u><br>This read across case does not follow a reviewed AOP. However, data exist that could support the proposed AOP for our suggested positive compound (Antimycin A). |
| | medium (since AOP is medium) | <u>Key events reflected by assays</u><br>However, the used assays are partly linked to the existing AOP concerning complex I inhibition leading to parkinsonian liabilities. Some of the key events addressed in this specific AOP are also used in the proposed AOP. Most uncertainty lies in the fact that it is not sure that the used NAMs can be used to assess the proposed adverse outcome; neurotoxicity. |
| Similarity of endpoint data (among source compounds) | Low | The *in vivo* neurotoxicity data on the source compounds unequivocally shows no sign of neurotoxicity. In one case, there is no specific repeat-dose neurotoxicity study, but from the other repeat-dose studies there is no signal. |
| Concordance and weight of evidence | Low/ | Although, the chemical similarity between the target and source compounds and within source compounds is not high they share a similar toxophore and also 3D structure. Therefore, concerning the impact on toxicodynamics, they are considered structurally identical/ very similar, |

| | | |
|---|---|---|
| | | which is supported by the absence of neurotoxicity *in vivo*. The uncertainty for the identification of neurotoxicity is therefore considered low. The structural variability in the molecules potentially have an impact on the toxicokinetics. However, since they appear to have similar ADME properties, the overall uncertainty due to kinetic differences is considered low-medium.<br>When tested across the different assays and endpoint there is high concordance in the result between the target and the source compounds.<br>Overall, the target compound is biologically comparable to the source compounds and there is high concordance.<br>The target compound and the source compounds are biologically active and inhibit early key events. The target compound was negative in the neurite outgrowth assay in SH-SY5Y cells, while some of the source compounds showed weak effects (thus reducing the uncertainty of the hypothesis).Neither the target and the source compounds were regarded as neurotoxic in the neuritetox assay in LUHMES cells.<br>Read across of negative effects gives uncertainty since the sensitivity of any test system (including *in vivo* animal studies) can be questioned. To mitigate this uncertainty the positive compound Antimycin have also been tested, to give an indication of the sensitivity of the given test system. |
| Overall | Low/medium | Overall, the uncertainty of this approach is considered low to medium. This assessment is based on the medium uncertainty for the prediction of the kinetic comparison of the target compound azoxystrobin and the source compounds, the low uncertainty for the toxicodynamic similarity of target and source compounds based on NAM data as well as the toxicodynamic difference to the reference compound antimycin A, and finally on the absence of any signs of neurotoxicity from repeated dose toxicity studies including designated neurotoxicity studies for the different source compounds.<br>The highest remaining uncertainty is connected to the fact that higher plasma peak concentrations are predicted for azoxystrobin as compared to the other strobilurines even though the predicted kinetic difference can be regarded as within *in vivo* variability. |

## 6.2. Integrated conclusion

The assumption for this read across case is that the target compound azoxystrobin has no TG424 data, however, the source compounds do not show signs of neurotoxicity neither in repeated dose toxicity studies nor in designated neurotoxicity studies (acute to sub-chronic).

The scientific **hypothesis** is: Can the absence of a neurotoxic potential mediated by inhibition of complex III of the mitochondria for azoxystrobin be predicted by toxicodynamic and toxicokinetic NAM data?

The hypothesis is supported by mechanistic data, anchored to a putative AOP based on the MIE inhibition of the mitochondrial CIII complex leading to neurotoxicity as shown *in vivo* for the reference compound antimycin A.

The overall structural similarity of the compounds is low, however the target and source compounds share an identical toxophore which is resulting in the same pesticidal mode of action and they also are predicted to have similar 3D structure. The differences in the remaining structure might be the cause for slight differences in the *in vivo* kinetic data and some differences in the *in vitro* kinetic and PBTK data gained in this project (probably primarily due the lower logP of azoxystrobin as compared to the other strobilurins). The kinetic data and simulations confirm similar kinetics and that the exposure to the brain is limited being maximally twice the plasma koncentration. However, since one consequence of this kinetic data is a predicted higher plasma peak concentration of azoxystrobin as compared to the other strobilurins, this results in some remaining uncertainty concerning the toxicokinetic similarity within this read across, even though the predicted kinetic difference can be regarded as within *in vivo* variability. Ultimately, if necessary, this uncertainty could be mitigated by a single-dose toxicokinetic *in vivo* study rather than a TG424 study.

The read across hypothesis is supported by the NAM data generated in EU-ToxRisk. The inhibition of CIII complexes, measured by oxygen consumption, by the target compound azoxystrobin seemed to be slightly less strong than by the source compounds pyraclostrobin and picoxystrobin, while the antimycin A resulted in a much stronger inhibition. This was confirmed with whole cells as well. Effects on membrane potential were marked by Antimycin A and orders of magnitude less with the target and source compounds. Effects on glycolysis and cell viability were similar between the compounds. The target compound was negative in the neurite outgrowth assay in SH-SY5Y cells, while some of the source compounds showed weak effects. Neither the target and the source compounds were regarded as neurotoxic in the neuritetox assay in LUHMES cells.

Overall, based on the generated data on kinetics and effect data, a neurotoxic potential of azoxystrobin mediated by a complex III inhibitory mode of action can be excluded.

# 7. Acknowledgements

The case study was part of the EU ToxRisk project. The core authors of this case study document are Susanne Hougaard Bennekou[1], Wanda van der Stel[2], Giada Carta[3], Julie Eakins[4], Johannes Delp[5], Anna Forsby[6], Hennicke Kamp[7], Ian Gardner[8], Barbara Zdradil[9], Manual Pastor[10], Jose Carlos Gomes[10], Andrew White[11], Thomas Steger-Hartman[12], Erik H.J. Danen[2], Marcel Leist[5], Paul Walker[4], Paul Jennings[3], Bob van de Water[2].

[1] National Food Institute, Technical University of Denmark (DTU), Lyngby, Denmark

[2] Division of Drug Discovery and Safety, Leiden Academic Centre of Drug Research, Leiden University, Leiden, the Netherlands.

[3] Division Molecular and Computational Toxicology, Vrije University Amsterdam, Amsterdam, the Netherlands.

[4] Cyprotex Discovery Ltd., Alderley Park, Macclesfield, Cheshire, United Kingdom.

[5] University of Konstanz, Konstanz, Germany.

[6] Department of Biochemistry and Biophysics, Stockholm University, Stockholm, Sweden.

[7] BASF, Ludwigshafen, Germany.

[8] Certara UK Limited, Sheffield, United Kingdom.

[9] University of Vienna, Austria.

[10] Universitat Pompeu Fabra, Spain.

[11] Unilever, Bedfordshire, United Kingdom.

[12] Bayer, Berlin, Germany.

# 8. References


Bartlett, D. W., Clough, J. M., Godwin, J. R., Hall, A. A., Hamer, M., & Parr-Dobrzanski, B. (2002). The strobilurin fungicides. *Pest Management Science*, Vol. 58, No. 7, pp. 649–662. https://doi.org/10.1002/ps.520

Berry, E. A., De Bari, H., & Huang, L.-S. (2013). Unanswered questions about the structure of cytochrome bc1 complexes. *Biochimica et Biophysica Acta (BBA) - Bioenergetics*, Vol. 1827, No. 11–12, pp. 1258–1277. https://doi.org/10.1016/j.bbabio.2013.04.006

Berry, E. A., & Huang, L.-S. (2011). Conformationally linked interaction in the cytochrome bc1 complex between inhibitors of the $Q_o$ site and the Rieske iron–sulfur protein. *Biochimica et Biophysica Acta (BBA) - Bioenergetics*, Vol. 1807, No. 10, pp. 1349–1363. https://doi.org/10.1016/J.BBABIO.2011.04.005

Blakely, E. L., Mitchell, A. L., Fisher, N., Meunier, B., Nijtmans, L. G., Schaefer, A. M., Taylor, R. W. (2005). A mitochondrial cytochrome b mutation causing severe respiratory chain enzyme deficiency in humans and yeast. *FEBS Journal*, Vol. 272, No. 14, pp. 3583–3592. https://doi.org/10.1111/j.1742-4658.2005.04779.x

Bywood, P. T., & Johnson, S. M. (2003). Mitochondrial Complex Inhibitors Preferentially Damage Substantia Nigra Dopamine Neurons in Rat Brain Slices. *Experimental Neurology*, Vol. 179, No. 1, pp. 47–59. https://doi.org/10.1006/EXNR.2002.8044

Cao, F., Wu, P., Huang, L., Li, H., Qian, L., Pang, S., & Qiu, L. (2018). Short-term developmental effects and potential mechanisms of azoxystrobin in larval and adult zebrafish (*Danio rerio*). *Aquatic Toxicology*, Vol. 198, pp. 129–140. https://doi.org/10.1016/j.aquatox.2018.02.023

Chang TI, Horal M, Jain SK, Wang F, Patel R, Loeken MR. (2003). Oxidant regulation of gene expression and neural tube development: Insights gained from diabetic pregnancy on molecular causes of neural tube defects. *Diabetologia*. Vol. 46, No. 4, pp. 538-545. doi:10.1007/s00125-003-1063-2

Conboy E, Selcen D, Brodsky M, Gavrilova R, Ho ML. (2018). Novel Homozygous Variant in TTC19 Causing Mitochondrial Complex III Deficiency with Recurrent Stroke-Like Episodes: Expanding the Phenotype. *Semin Pediatr Neurol*, Vol. 26, pp. 16-20. doi:0.1016/j.spen.2018.04.003.

Delp J, Gutbier S, Klima S, *et al.* (2018). A high-throughput approach to identify specific neurotoxicants/ developmental toxicants in human neuronal cell function assays [published correction appears in *ALTEX*. Vol. 36, No. 3, pp. 505]. *ALTEX*. Vol. 35, No. 2, pp. 235-253. doi:10.14573/altex.1712182

Durant JL, Leland BA, Henry DR, Nourse JG. (2002). Reoptimization of MDL keys for use in drug discovery. *J Chem Inf Comput Sci.* Vol. 42, No. 6, pp. 1273-1280. doi:10.1021/ci010132r

EFSA (2013). Scientific Opinion on the developmental neurotoxicity potential of acetamiprid and imidacloprid. EFSA Journal, Vol. 11, No. 12. European Food Safety Authority, Parma. https://doi.org/10.2903/j.efsa.2013.3471

Esser, C., Scheffner, M., & Höhfeld, J. (2005). The chaperone-associated ubiquitin ligase CHIP is able to target p53 for proteasomal degradation. *The Journal of Biological Chemistry*, Vol. 280, No. 29, pp. 27443–8. https://doi.org/10.1074/jbc.M501574200

Esser L, Quinn B, Li YF, *et al.* (2004). Crystallographic studies of quinol oxidation site inhibitors: a modified classification of inhibitors for the cytochrome bc(1) complex. *J Mol Biol.*, Vol. 341, No. 1, pp. 281–302. doi:10.1016/j.jmb.2004.05.065

Flampouri, E., Theodosi-Palimeri, D., & Kintzios, S. (2018). Strobilurin fungicide kresoxim-methyl effects on a cancerous neural cell line: oxidant/antioxidant responses and *in vitro* migration. *Toxicology Mechanisms and Methods*, Vol. 28, Nol. 9, pp. 709–716. https://doi.org/10.1080/15376516.2018.1506848

Gao, A.-H., Fu, Y.-Y., Zhang, K.-Z., Zhang, M., Jiang, H.-W., Fan, L.-X., Li, J.-Y. (2014). Azoxystrobin, a mitochondrial complex III $Q_o$ site inhibitor, exerts beneficial metabolic effects *in vivo* and *in vitro*. *Biochimica et Biophysica Acta (BBA) - General Subjects*, Vol. 1840, No. 7, pp. 2212–2221. https://doi.org/10.1016/j.bbagen.2014.04.002

Ghezzi D, Arzuffi P, Zordan M, Da Re C, Lamperti C, Benna C, D'Adamo P, Diodato D, Costa R, Mariotti C, Uziel G, Smiderle C, Zeviani M. (2011). Mutations in TTC19 cause mitochondrial complex III deficiency and neurological impairment in humans and flies. *Nat Genet*, Vol. 43, No. 3, pp. 259-63. doi: 10.1038/ng.761.

Hatefi, Y. (1985). The Mitochondrial Electron Transport and Oxidative Phosphorylation System. *Annual Review of Biochemistry*, Vol. 54, No. 1, pp. 1015–1069. https://doi.org/10.1146/annurev.bi.54.070185.005055

Huang, L.-S., Cobessi, D., Tung, E. Y., & Berry, E. A. (2005). Binding of the respiratory chain inhibitor antimycin to the mitochondrial bc1 complex: a new crystal structure reveals an altered intramolecular hydrogen-bonding pattern. *Journal of Molecular Biology*, Vol. 351, No. 3, pp. 573–97. https://doi.org/10.1016/j.jmb.2005.05.053

Hytti M, Korhonen E, Hyttinen JMT, Roehrich H, Kaarniranta K, Ferrington DA, Kauppinen A. (2019). Antimycin A-Induced Mitochondrial Damage Causes Human RPE Cell Death despite Activation of Autophagy. *Oxid Med Cell Longev*. Vol. 2019, Article ID 1583656, 12 pp. https://doi.org/10.1155/2019/1583656. eCollection 2019.

Im, A. R., Kim, Y. H., Uddin, M. R., Chae, S. W., Lee, H. W., Jung, W. S., Lee, M. Y. (2013). Protection from antimycin A-induced mitochondrial dysfunction by Nelumbo nucifera seed extracts. *Environmental Toxicology and Pharmacology*, Vol. 36, No. 1, pp. 19–29. https://doi.org/10.1016/j.etap.2013.02.015

Jang, Y., Kim, J.-E., Jeong, S.-H., Paik, M.-K., Kim, J. S., & Cho, M.-H. (2016). Trifloxystrobin-induced mitophagy through mitochondrial damage in human skin keratinocytes. *The Journal of Toxicological Sciences*, Vol. 41, No. 6, pp. 731–737. https://doi.org/10.2131/jts.41.731.

Krug AK, Balmer NV, Matt F, Schönenberger F, Merhof D, Leist M. (2013). Evaluation of a human neurite growth assay as specific screen for developmental neurotoxicants. *Arch Toxicol*., Vol. 87, No. 12, pp. 2215-31. doi: 10.1007/s00204-013-1072-y.

Kunii M1, Doi H1, Higashiyama Y, Kugimoto C, Ueda N, Hirata J, Tomita-Katsumoto A, Kashikura-Kojima M, Kubota S, Taniguchi M, Murayama K, Nakashima M, Tsurusaki Y, Miyake N, Saitsu H, Matsumoto N, Tanaka F. (2015). A Japanese case of cerebellar ataxia, spastic paraparesis and deep sensory impairment associated with a novel homozygous TTC19 mutation. *J Hum Genet*., Vol. 60, No. 4, pp. 187-91.

Lai B, Zhang L, Dong LY, Zhu YH, Sun FY, Zheng P. (2005). Inhibition of Qi site of mitochondrial complex III with antimycin A decreases persistent and transient sodium currents via reactive oxygen species and protein kinase C in rat hippocampal CA1 cells. *Exp Neurol.* Vol. 194, No. 2, pp. 484-494. doi:10.1016/j.expneurol.2005.03.005

Leist M, Ghallab A, Graepel R, Marchan R, Hassan R, Bennekou SH, Limonciel A, Vinken M, Schildknecht S, Waldmann T, Danen E, van Ravenzwaay B, Kamp H, Gardner I, Godoy P, Bois FY, Braeuning A, Reif R, Oesch F, Drasdo D, Höhme S, Schwarz M, Hartung T, Braunbeck T, Beltman J, Vrieling H, Sanz F, Forsby A, Gadaleta D, Fisher C, Kelm J, Fluri D, Ecker G, Zdrazil B, Terron A, Jennings P, van der Burg B, Dooley S, Meijer AH, Willighagen E, Martens M, Evelo C, Mombelli E, Taboureau O, Mantovani A, Hardy B, Koch B, Escher S, van Thriel C, Cadenas C, Kroese D, van de Water B, Hengstler JG. (2017). Adverse outcome pathways: opportunities, limitations and open questions. *Arch Toxicol*. Vol. 91, No. 11, pp. 3477-3505.

Li, H., Cao, F., Zhao, F., Yang, Y., Teng, M., Wang, C., & Qiu, L. (2018). Developmental toxicity, oxidative stress and immunotoxicity induced by three strobilurins (pyraclostrobin, trifloxystrobin and picoxystrobin) in zebrafish embryos. *Chemosphere*, Vol. 207, pp. 781–790. https://doi.org/10.1016/j.chemosphere.2018.05.146

Luz, A. L., Kassotis, C. D., Stapleton, H. M., & Meyer, J. N. (2018). The high-production volume fungicide pyraclostrobin induces triglyceride accumulation associated with mitochondrial dysfunction, and promotes adipocyte differentiation independent of PPARγ activation, in 3T3-L1 cells. *Toxicology*, Vol. 393, pp. 150–159. https://doi.org/10.1016/j.tox.2017.11.010

Ma X, Jin M, Cai Y, Xia H, Long K, Liu J, Yu Q, Yuan J. (2011). Mitochondrial electron transport chain complex III is required for antimycin A to inhibit autophagy. *Chem Biol.,* Vol. 18, No. 11, pp. 1474-81. https://doi.org/10.1016/j.chembiol.2011.08.009.

Meunier, B., Fisher, N., Ransac, S., Mazat, J.-P., & Brasseur, G. (2013). Respiratory complex III dysfunction in humans and the use of yeast as a model organism to study mitochondrial myopathy and associated diseases. *BBA - Bioenergetics*, Vol. 1827, pp. 1346–1361. https://doi.org/10.1016/j.bbabio.2012.11.015

Mordaunt DA, Jolley A, Balasubramaniam S, Thorburn DR, Mountford HS, Compton AG, Nicholl J, Manton N, Clark D, Bratkovic D, Friend K, Yu S. Am J Med Genet A. (2015). Phenotypic variation of TTC19-deficient mitochondrial complex III deficiency: a case report and literature review. Vol. 167, No. 6, pp. 1330-6. doi: 10.1002/ajmg.a.36968.

Ockleford, C., Adriaanse, P., Berny, P., Brock, T., Duquesne, S., Grilli, S., Hernandez-Jerez, A. F. (2017). Scientific Opinion of the PPR Panel on the follow-up of the findings of the External Scientific Report "Literature review of epidemiological studies linking exposure to pesticides and health effects", *EFSA Journal*, Vol. 15, No. 10, pp. 5007, 101pp. EFSA Panel on Plant Protection Products and their Residues, Parma. https://doi.org/10.2903/j.efsa.2017.5007

OECD (2018a), Adverse Outcome Pathway on Inhibition of the mitochondrial complex I of nigro-striatal neurons leading to parkinsonian motor deficits, OECD Series on Adverse Outcome Pathways, No. 7, OECD Publishing, Paris, https://doi.org/10.1787/b46c3c00-en.

OECD (2018b), Harmonised template 201: Intermediate effects. *Non-apical observations during in vitro testing, i.e. intermediate effects on molecular, subcellular, cell, tissue or organ level that can be relevant to the hazard assessment (and possibly inform the adverse outcome pathways)*. Last update: Dec. 2018. https://www.oecd.org/ehs/templates/harmonised-templates-intermediate-effects.htm

Pauwels, P. J., Opperdoes, F. R., & Trouet, A. (1985). Effects of Antimycin, Glucose Deprivation, and Serum on Cultures of Neurons, Astrocytes, and Neuroblastoma Cells. *Journal of Neurochemistry*. Vol. 44, No. 1, pp. 143–148. https://doi.org/10.1111/j.1471-4159.1985.tb07123.x

Pearson, B. L., Simon, J. M., McCoy, E. S., Salazar, G., Fragola, G., & Zylka, M. J. (2016). Identification of chemicals that mimic transcriptional changes associated with autism, brain aging and

neurodegeneration. *Nature Communications*, Vol. 7, No. 11173. https://doi.org/10.1038/ncomms11173

Patterson DE, Cramer RD, Ferguson AM, Clark RD, Weinberger LE. (1996). Neighborhood behavior: a useful concept for validation of "molecular diversity" descriptors. *J Med Chem*. Vol. 39, No. 16, pp. 3049-3059. doi:10.1021/jm960290n

Regueiro, J., Olguín, N., Simal-Gándara, J., & Suñol, C. (2015). Toxicity evaluation of new agricultural fungicides in primary cultured cortical neurons. *Environmental Research*, Vol. 140, pp. 37–44. https://doi.org/10.1016/J.ENVRES.2015.03.013

Rodrigues, E. T., Pardal, M. Â., Laizé, V., Cancela, M. L., Oliveira, P. J., & Serafim, T. L. (2015). Cardiomyocyte H9c2 cells present a valuable alternative to fish lethal testing for azoxystrobin. *Environmental Pollution (Barking, Essex : 1987)*, Vol. 206, pp. 619–26. https://doi.org/10.1016/j.envpol.2015.08.026

SAPEA (2018). Improving authorisation processes for plant protection products in Europe: a scientific perspective on the potential risks to human health. Science Advice for Policy by European Academies, Berlin. https://doi.org/10.26356/plantprotectionproducts.

Schreyer, A. M., & Blundell, T. (2012). USRCAT: real-time ultrafast shape recognition with pharmacophoric constraints. *Journal of Cheminformatics*, Vol. 4, No. 1, No. 27. https://doi.org/10.1186/1758-2946-4-27

Shi, X.-K., Bian, X.-B., Huang, T., Wen, B., Zhao, L., Mu, H.-X., Lin, C.-Y. (2017). Azoxystrobin Induces Apoptosis of Human Esophageal Squamous Cell Carcinoma KYSE-150 Cells through Triggering of the Mitochondrial Pathway. *Frontiers in Pharmacology*, Vol. 8, No. 277. https://doi.org/10.3389/fphar.2017.00277.

Shin YS, Ryall JG, Britto JM, Lau CL, Devenish RJ, Nagley P, Beart PM. (2019). Inhibition of bioenergetics provides novel insights into recruitment of PINK1-dependent neuronal mitophagy. *J Neurochem*. Vol. 149, No. 2, pp. 269-283. http://doi.org/10.1111/jnc.14667. Epub 2019 Feb 12.

Simon JM, Paranjape SR, Wolter JM, Salazar G, Zylka MJ. (2019). High-throughput screening and classification of chemicals and their effects on neuronal gene expression using RASL-seq. *Sci Rep.*, Vol. 9, No. 1, pp. 4529. doi: 10.1038/s41598-019-39016-5.

Stiegler NV, Krug AK, Matt F, Leist M. (2011). Assessment of chemical-induced impairment of human neurite outgrowth by multiparametric live cell imaging in high-density cultures. *Toxicol Sci*., Vol. 121, No. 1, pp. 73-87. doi: 10.1093/toxsci/kfr034.

Suh, K. S., Lee, Y. S., Seo, S. H., Kim, Y. S., & Choi, E. M. (2013). Gold nanoparticles attenuates antimycin A-induced mitochondrial dysfunction in MC3T3-E1 osteoblastic cells. *Biological Trace Element Research*, Vol. 153, No. 1–3, pp. 428–436. https://doi.org/10.1007/s12011-013-9679-7.

Terron A, Bal-Price A, Paini A, Monnet-Tschudi F, Bennekou SH; EFSA WG EPI1 Members, Leist M, Schildknecht S. (2018). Adverse outcome pathway for the development of parkinsonian motor deficits by mitochondrial complex I inhibition. *Arch Toxicol.*, Vol. 92, No. 1, pp. 41-82.

Tokutake, N., Miyoshi, H., Satoh, T., Hatano, T., & Iwamura, H. (1994). Structural factors of antimycin A molecule required for inhibitory action. *Biochimica et Biophysica Acta (BBA) - Bioenergetics*, Vol. 1185, No. 3, pp. 271–278. https://doi.org/10.1016/0005-2728(94)90241-0.

U.S. EPA (2016), Halauxifen-methyl - New Active Ingredient Human Health Risk Assessment for Proposed Uses on Cereal Grains (Barley, Wheat, and Triticale). DP Barcode: D406145, EPA-HQ-OPP-2012-0919-0005, United States Environmental Protection Agency, Washington D.C. https://www.regulations.gov/document?D=EPA-HQ-OPP-2012-0919-0005.

Xia D, Yu CA, Kim H, *et al.* (1997). Crystal structure of the cytochrome bc1 complex from bovine heart mitochondria [published correction appears in *Science,* Vol. 278, No. 5346, pp. 2037]. *Science*. Vol. 277, No. 5322, pp. 60-66. doi:10.1126/science.277.5322.60

Xia, M., Huang, R., Shi, Q., Boyd, W. A., Zhao, J., Sun, N., Simeonov, A. (2018). Comprehensive Analyses and Prioritisation of Tox21 10K Chemicals Affecting Mitochondrial Function by in-Depth Mechanistic Studies. *Environmental Health Perspectives*, Vol. 126, No. 7, CID. 077010. https://doi.org/10.1289/EHP2589.

Zhang, L., Yu, L., & Yu, C. A. (1998). Generation of superoxide anion by succinate-cytochrome c reductase from bovine heart mitochondria. *The Journal of Biological Chemistry*, Vol. 273, No. 51, pp. 33972–6. https://doi.org/10.1074/JBC.273.51.33972.

Zheng, X., Boyer, L., Jin, M., Kim, Y., Fan, W., Bardy, C., Hunter, T. (2016). Alleviation of neuronal energy deficiency by mtor inhibition as a treatment for mitochondria-related neurodegeneration. *eLife,* Vol. 5, ID e13378. https://doi.org/10.7554/eLife.13378

# Appendix: data matrix

| Chemical ID | | | | | | | |
|---|---|---|---|---|---|---|---|
| | | Target | Source1 | Source2 | Source3 | Source4 | Reference |
| CAS | | 131860-33-8 | 175013-18-0 | 117428-22-5 | 141517-21-7 | 143390-89-0 | 1397-94-0 |
| Name | | Azoxystrobin | Pyraclostrobin | Picoxystrobin | Trifloxystrobin | Kresoxim-methyl | Antimycin A |
| Structure | | 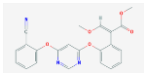 | 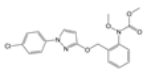 | 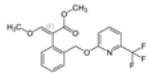 | 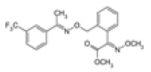 | 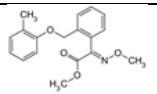 | 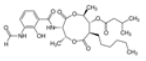 |
| SMILE code | | CO/C=C(/C(=O)OC)c1ccccc1Oc1cc(Oc2ccccc2C#N)ncn1 | COC(=O)N(OC)c1ccccc1COc1ccn(-c2ccc(Cl)cc2)n1 | CO/C=C(/C(=O)OC)c1ccccc1COc1cccc(C(F)(F)F)n1 | CO/N=C(/C(=O)OC)c1ccccc1CON=C(C)c1cccc(C(F)(F)F)c1 | CO/N=C(/C(=O)OC)c1ccccc1COc1ccccc1C | CCCCCC[C@H]1C(=O)O[C@H](C)[C@H](NC(=O)c2cccc(NC=O)c2O)C(=O)O[C@@H](C)[C@@H]1OC(=O)CC(C)C |
| Summary of data gap filling | | | | | | | |
| | | Target | Source 1 | Source2 | Source3 | Source4 | Reference |
| Target endpoint (low neurotoxic potential) | Experimental result | | | | | | |
| | **Integrated conclusion (e.g. read-across)** | TG424 | | | | | |
| Physical-chemical data | | | | | | | |
| logPow (measured value) | | 2.5 | 3.99 | 3.68 | 4.5 | 3.4 | No measured value |
| logPow (calculated value) | | 3.7 | 4.1 | 3.6 | 4.9 | 4.1 | 4.75 |
| Similarity (Tanimoto Coefficient | | | 0.52 | 0.3 | 0.69 | 0.53 | 0.56 |
| Similarity 3D | | | 0.76 | 0.65 | 0.7 | 0.61 | |
| Kinetics** *In vivo /in silico* | | | | | | | |
| Absorption | | High/High | Moderate/Moderate | High/high | Low/low | Ow/moderate | No data/low |
| Distribution | | Moderate (2 times Pl. C) /Moderate | Moderate/Moderate | Not measured/Moderate | Low/moderate | Low/moderate | No data/moderate |

| | | | | | | | |
|---|---|---|---|---|---|---|---|
| Metabolism | | Extensive/Extensive | Extensive/Extensive | Extensive/Extensive | Extensive/Extensive | Extensive/Extensive | No data/Extensive |
| Excretion | | High/Moderate | Moderate/low | high/low | Extensive/low | High/moderate | No data/low |
| Supporting data related to the target endpoint(s) | | | | | | | |
| | | Target | Source1 | Source2 | Source3 | Source4 | Reference |
| *In vivo* | Neuro | | Not detected in acute and repeat-dose neurotox. studies | Not detected in standard repeat-dose studies. No neurotox. Studies available | Not detected in acute neurotox study and neurotox. Evaluation of 90 day repeat study | Not detected in acute and repeat-dose neurotox. studies | |
| *In vitro* (BMC25 [nM]) | Alternative method A | | | | | | |
| | Oxygen consumption (not tested in concentration-response) (intact cells LHUMES _24h) | ≤ 50000 | ≤ 50000 | ≤ 50000 | ≤ 50000 | ≤ 12500 | 500 |
| | Oxygen consumption neuro (not tested in concentration-response) (complexes LHUMES _24h) | ≤ 50000 | ≤ 50000 | ≤ 50000 | not tested | not tested | ≤ 50000 |
| | Oxygen consumption (HepG2_24h) | 3610 | 469 | 518 | 2000 | >10000 | not tested |
| | Mitochondrial membrane potential (HepG2_24h) | 1122 | 288 | 389 | NA | NA | 3 |
| | Mitochondrial membrane potential (RPTEC/TERT1_24h) | NA | 79 | NA | 2570 | NA | 0.8 |
| | Mitochondrial membrane potential (SH-SY5Y_24h) | 3234 | 2951 | 8318 | 363 | 1349 | 63 |
| | Lactate production (HepG21_24h) | 2435 | 179 | 475 | 9224 | 119 | 72 |
| | Lactate production (RPTEC/TERT1_24h) | 971 | 246 | 331 | 1572 | >10000 | 174 |
| | Lactate production (SH-SY5Y_24h) | (+) | + | (+) | (+) | - | + |
| | Cytotoxicity (resazurin)) (HepG2_24h) | >10000 | >10000 | >10000 | >10000 | >10000 | >10000 |
| | Cytotoxicity (resazurin)) (RPTEC/TERT1_24h) | 5012 | 437 | 871 | 6026 | 776 | 36 |
| | Cytotoxicity (resazurin)) (SH-SY5Y_24h) | >10000 | >10000 | >10000 | >10000 | >10000 | >10000 |

| | | | | | | | |
|---|---|---|---|---|---|---|---|
| | Cytotoxicity (resazurin)) (LHUMES_24h) | >50000 | >50000 | >50000 | >50000 | >50000 | 25703 |
| | Neurite outgrowth (LUHMES_single) | 31623 | 17378 | 48978 | 18197 | 41687 | 17378 |
| | Neurite degeneration (LUHMES_repeat) | 19851 | 3872 | 16040 | not tested | not tested | 7881 |
| | ATP content (SH-SY5Y_120h) | 4467 | 166 | 1622 | 1175 | 3631 | 0,955 |
| | Neurite degeneration (SH-SY5Y_24h/120h) | >10000/>10000 | >10000/3090 | >10000/>10000 | >10000/2089 | >10000/7762 | 7244/6166 |
| | Cytotoxicity (SH-SY5Y_24h/120h) | >10000/>10000 | >10000/5012 | >10000/8912 | >10000/>10000 | >10000/>10000 | >10000/3802 |
| | Lactate production (RPTEC/TERT1_5days) (EC20) | 70 | 22 | 30 | not tested | not tested | 16 |

* More relevant metabolite in comparison to parent (e.g., if metabolite is more toxic than the parent or shows the toxicity defining the critical effect)

**General outline of relative comparative kinetics

# Annex I. Methods

**Please refer to the separate publication for the detailed methods in Annex 1: ENV/JM/MONO(2020)23/ANN1**

Seahorse

- Complexes
- Whole cells

Mitochondrial Membrane Potential

Mitochondrial viability

- lactate
- resazurin

Neurite outgrowth

- glucose
- galactose

Bioavailability

- model
- samples
- mass spectrometry

PBPK

Repeat dosing

Receptor docking

Chemical similarity

- 3D-modeling
- Tanimoto coefficients

Some methods are still in the process of being described, see attached overview below

Addendum Excel table